

**Phosphine Substitution and Linkage Isomerization in CpRu(PPh<sub>3</sub>)<sub>2</sub>NCS and CpRu(PPh<sub>3</sub>)<sub>2</sub>SeCN**

Duy-Khoi Dang<sup>a</sup>, Damla Cehreli, <sup>a</sup> Benjamin S. Rich<sup>a</sup>, Terry E. Haas <sup>b</sup>, Frank R. Fronczek,<sup>c</sup> and Rein U. Kirss<sup>\*a</sup>

<sup>a</sup>Department of Chemistry and Chemical Biology Northeastern University, Boston MA 02115.

<sup>b</sup>Department of Chemistry Tufts University, Medford MA 02155.

<sup>c</sup> Department of Chemistry Louisiana State University, Baton Rouge, LA 70803

**Experimental Details**

General Procedures	S4
Synthesis of <b>2a</b> .	S4
Synthesis of <b>2b</b> .	S4
Synthesis of <b>3b</b> .	S5
Synthesis of <b>4b</b> .	S5
Kinetic Measurements	S6
<b>Computational Methods</b>	S6
<b>Figure S1:</b> (a) <sup>1</sup> H NMR spectrum of <b>1a</b> in CDCl <sub>3</sub> .	S8
(b) <sup>31</sup> P NMR spectrum of <b>1a</b> in CDCl <sub>3</sub> .	
<b>Figure S2:</b> (a) <sup>1</sup> H NMR spectrum of <b>2a</b> in CDCl <sub>3</sub> .	S9
(b) <sup>31</sup> P NMR spectrum of <b>2a</b> in CDCl <sub>3</sub> .	
(c) <sup>1</sup> H NMR spectrum of CDCl <sub>3</sub> containing 0.03% v/v TMS.	
<b>Figure S3:</b> (a) Best molecular structure of <b>2b</b> .	S10
(b) Two superimposed orientations of <b>4b</b> showing the mirror-related disorder in the structure.	
<b>Figure S4:</b> (a) <sup>1</sup> H NMR spectrum of <b>2b</b> in CDCl <sub>3</sub> .	S11
(b) <sup>31</sup> P NMR spectrum of <b>2b</b> in CDCl <sub>3</sub> .	
(c) <sup>31</sup> P NMR of a mixture of <b>2a</b> and <b>2b</b> in CDCl <sub>3</sub> .	
<b>Figure S5:</b> (a) Reaction of CpRu(PPh <sub>3</sub> ) <sub>2</sub> Cl with SCN <sup>-</sup> in THF @ 47°C.	S12
(b) isomerization of <b>2b</b> to <b>2a</b> with SCN <sup>-</sup> in THF/10% C <sub>6</sub> D <sub>6</sub> @ 40°C.	
<b>Figure S6:</b> (a) <sup>1</sup> H NMR spectrum of <b>3b</b> in C <sub>6</sub> D <sub>6</sub> .	S13
(b) <sup>31</sup> P NMR spectrum of <b>3b</b> in C <sub>6</sub> D <sub>6</sub> .	
<b>Figure S7:</b> (a) <sup>1</sup> H NMR spectrum of <b>4b</b> in CDCl <sub>3</sub> .	S14
(b) <sup>31</sup> P NMR spectrum of <b>4b</b> in CDCl <sub>3</sub> .	
<b>Figure S8:</b> (a) <sup>31</sup> P NMR spectrum of <b>1a</b> (5 mM) + PMePh <sub>2</sub> (41 mM) in C <sub>6</sub> H <sub>5</sub> F/10% v/v C <sub>6</sub> D <sub>6</sub> at t=0.	S15
(b) <sup>31</sup> P NMR spectrum of <b>1a</b> + PMePh <sub>2</sub> in C <sub>6</sub> H <sub>5</sub> F/10% v/v C <sub>6</sub> D <sub>6</sub> after heating at 40°C for 317 h showing 75% conversion to <b>2a</b> with small amounts of <b>2b</b> .	
<b>Figure S9:</b> (a) <sup>31</sup> P NMR spectrum of <b>1a</b> (5 mM) + PMePh <sub>2</sub> (39 mM) in C <sub>6</sub> H <sub>5</sub> F/10% v/v C <sub>6</sub> D <sub>6</sub> after heating at 50°C for 21.5 h	S16

(b)  $^{31}\text{P}$  NMR spectrum of **1a** + PMePh<sub>2</sub> in C<sub>6</sub>H<sub>5</sub>F/10% v/v C<sub>6</sub>D<sub>6</sub> after heating at 50°C for 150 h showing 96% conversion to **2a**.

**Figure S10:** (a)  $^{31}\text{P}$  NMR spectrum of **1a** (7 mM) + PMePh<sub>2</sub> (76 mM) in THF/10% v/v C<sub>6</sub>D<sub>6</sub> at t=0 s. S17

(b)  $^{31}\text{P}$  NMR spectrum of **1a** + PMePh<sub>2</sub> in THF/10% v/v C<sub>6</sub>D<sub>6</sub> after heating at 40°C for 500 h.

**Figure S11:** Concentration Changes in the Reaction Between **1a** and PMePh<sub>2</sub> in THF/10% C<sub>6</sub>D<sub>6</sub> @ 40°C. S18

**Figure S12:** Representative plots of  $\ln[\text{CpRu}(\text{PPh}_3)_2\text{NCS}]$  vs t for the reaction between **1a** and PMePh<sub>2</sub> in (a) THF/10% C<sub>6</sub>D<sub>6</sub> and (b) C<sub>6</sub>H<sub>5</sub>F/10% C<sub>6</sub>D<sub>6</sub>. S19

**Figure S13:** Eyring plot for the reaction between **1a** and PMePh<sub>2</sub> in (a) THF/10% C<sub>6</sub>D<sub>6</sub>, (b) C<sub>6</sub>H<sub>5</sub>F/10% C<sub>6</sub>D<sub>6</sub> and (c) Plot of  $1/k_{obs}$  vs [PPh<sub>3</sub>] at 40°C in THF/10% C<sub>6</sub>D<sub>6</sub>. S20

**Figure S14:** Concentration Changes in the Reaction Between **1a**, PMePh<sub>2</sub>, and SCN<sup>-</sup> in (a) THF/10% C<sub>6</sub>D<sub>6</sub> @ 40°C and (b) C<sub>6</sub>H<sub>5</sub>F/10% C<sub>6</sub>D<sub>6</sub>. S21

**Figure S15:** (a)  $^{31}\text{P}$  NMR spectrum of **3b** (5.7 mM) + PMePh<sub>2</sub> (50 mM) in C<sub>6</sub>H<sub>5</sub>F/10% v/v C<sub>6</sub>D<sub>6</sub> at t=0 s S22

(b)  $^{31}\text{P}$  NMR spectrum of **3b** + PMePh<sub>2</sub> in C<sub>6</sub>H<sub>5</sub>F/10% v/v C<sub>6</sub>D<sub>6</sub> after heating at 30°C for 37.7 h.

**Figure S16:** Representative plots of  $\ln[\text{CpRu}(\text{PPh}_3)_2\text{SeCN}]$  vs t for the reaction between **1a** and PMePh<sub>2</sub> in C<sub>6</sub>H<sub>5</sub>F/10% C<sub>6</sub>D<sub>6</sub> and (b)  $k_{obs}$  vs [SeCN] @ 29°C S23

**Figure S17:** (a) Eyring plot for the reaction between **3b** and PMePh<sub>2</sub> in C<sub>6</sub>H<sub>5</sub>F/10% C<sub>6</sub>D<sub>6</sub>, (b) Plot of  $1/k_{obs}$  vs [PPh<sub>3</sub>] at 30°C in C<sub>6</sub>H<sub>5</sub>F/10% C<sub>6</sub>D<sub>6</sub>. S24

**Table S1:** Concentrations of reactants and products: CpRu(PPh<sub>3</sub>)<sub>2</sub>NCS (**1a**) + PMePh<sub>2</sub> in THF/C<sub>6</sub>D<sub>6</sub> @ 40°C (see Figure S10 for plots) S25

**Table S2:** Rate Constants for Phosphine Exchange: **1a** + PMePh<sub>2</sub>. S26

**Table S3:** Rate Constants for Phosphine Exchange: **3b** + PMePh<sub>2</sub>. S26

**Table S4.** Sample and crystal data for **1a**. S27

**Table S5.** Data collection and structure refinement for **1a**. S28

**Table S6.** Bond lengths (pm) for **1a**. S29

**Table S7.** Bond angles (°) for **1a**. S31

**Table S8.** Sample and crystal data for **2a**. S34

**Table S9.** Data collection and structure refinement for **2a**. S35

**Table S10.** Bond lengths (pm) for **2a**. S36

**Table S11.** Bond angles (°) for **2a**. S37

**Table S12.** Sample and crystal data for **3b**. S39

**Table S13.** Data collection and structure refinement for **3b**. S40

**Table S14.** Bond lengths (pm) for **3b**. S41

<b>Table S15.</b> Bond angles ( $^{\circ}$ ) for <b>3b</b> .	S43
<b>Table S16.</b> Sample and crystal data for <b>4b</b> .	S46
<b>Table S17.</b> Data collection and structure refinement for <b>4b</b> .	S47
<b>Table S18.</b> Bond lengths (pm) for <b>4b</b> .	S48
<b>Table S19.</b> Bond angles ( $^{\circ}$ ) for <b>4b</b> .	S50
<b>Derivation of the rate law</b>	S54
<b>References</b>	S55

## Experimental Details

Cyclopentadiene, RuCl<sub>3</sub>•xH<sub>2</sub>O, triphenylphosphine, methyldiphenylphosphine, KSCN, and KSeCN are commercially available (Fisher Acros). Solvents were purified by distillation from Na/benzophenone (C<sub>6</sub>D<sub>6</sub>, THF) or P<sub>2</sub>O<sub>5</sub> (CDCl<sub>3</sub>, C<sub>6</sub>H<sub>5</sub>F). All ruthenium compounds described in this work are air stable as solids, but their syntheses were performed under purified nitrogen atmospheres using Schlenk techniques or a M. I. Braun glove box. NMR spectra were recorded at 400 MHz for <sup>1</sup>H and 162 MHz for <sup>31</sup>P{<sup>1</sup>H} on a Mercury XL300 spectrometer. Proton chemical shifts are reported relative to residual protons in the solvent (CHCl<sub>3</sub> at 7.24 ppm and C<sub>6</sub>D<sub>5</sub>H at 7.15 ppm relative to TMS at 0.00 ppm). Phosphorus chemical shifts are reported relative to 85% H<sub>3</sub>PO<sub>4</sub> at 0.0 ppm. IR spectra were recorded as solids on a Bruker Astra ATR spectrometer equipped with ZnSe windows. Melting points were determined in capillary tubes using an Electrothermal 9110 or SRS Digimelt melting point apparatus and are uncorrected. Elemental analyses (C, H) were performed by Columbia Analytical Services, Inc. Tucson, AZ. Electrochemical measurements were made under nitrogen on a BAS 100 B/W electrochemical workstation or Pine electrochemical apparatus at 22°C using 1 x 10<sup>-3</sup> M solutions in dry CH<sub>2</sub>Cl<sub>2</sub>, 0.1 M <sup>n</sup>Bu<sub>4</sub>NPF<sub>6</sub> or <sup>n</sup>Bu<sub>4</sub>NBF<sub>4</sub> as supporting electrolyte at a scan rate of 100mV/s. The working electrode was a 3 mm Pt disk with a Pt wire as auxiliary electrode. A silver wire was used as a pseudo-reference electrode with ferrocene added as an internal standard. All potentials are referenced to ferrocene (E<sub>1/2</sub> = 0.00 V).

### Synthesis of CpRu(PPh<sub>3</sub>)<sub>2</sub>NCS (**1a**)

Cyclopentadienylrutheniumbis(triphenylphosphine)thiocyanate, CpRu(PPh<sub>3</sub>)<sub>2</sub>NCS **1a**, was prepared by literature procedures <sup>1</sup> from CpRu(PPh<sub>3</sub>)<sub>2</sub>Cl <sup>2</sup> and KSCN in methanol. Crystals suitable for X-ray crystallography were grown by slow evaporation of CH<sub>2</sub>Cl<sub>2</sub> solutions.

### Synthesis of CpRu(PPh<sub>3</sub>)(PMePh<sub>2</sub>)NCS (**2a**)

A solution of **1a** (106 mg, 0.141 mmols) and PMePh<sub>2</sub> (29 μL, 0.154 mmols) in 10 mL fluorobenzene was refluxed under nitrogen for 13 h. Solvent was evaporated under vacuum and the residue dissolved in CH<sub>2</sub>Cl<sub>2</sub>. The yellow-orange solution was passed through a thin pad of neutral alumina and the filtrate was layered with hexane. Cooling at -15°C yielded 87.7 mg (91%) of **2a**. The product was characterized by NMR and X-ray crystallography. Crystals of **2a**•CH<sub>2</sub>Cl<sub>2</sub> were grown by slow evaporation of a CH<sub>2</sub>Cl<sub>2</sub> solution. The yellow sample turns a mustard yellow color upon heating in a capillary and darkens to brown or black above 190°C. IR: ν<sub>CN</sub> = 2089 cm<sup>-1</sup>. <sup>1</sup>H (400 MHz, CDCl<sub>3</sub>): δ 7.0-7.6 (m, 25H, aryl), 5.30 (s, CH<sub>2</sub>Cl<sub>2</sub>), 4.22 (s, 5H, Cp), 1.07 (d, J = 8.8 Hz, 3H, CH<sub>3</sub>). <sup>31</sup>P{<sup>1</sup>H}(CDCl<sub>3</sub>): δ 46.0 (d, J=39 Hz), 32.6 (d, J=39 Hz); (THF) δ 47.0 ppm (d, J<sub>PP</sub>= 40 Hz), 34.1 (d, 40 Hz). Anal.

Calcd for C<sub>37</sub>H<sub>33</sub>NP<sub>2</sub>RuS: C, 64.71%; H, 4.86%. Found: C, 64.52%; H, 4.37%.

### Synthesis of CpRu(PPh<sub>3</sub>)(PMePh<sub>2</sub>)SCN (**2b**)

A slurry of CpRu(PPh<sub>3</sub>)(PMePh<sub>2</sub>)Cl<sup>3</sup> (106 mg, 0.49 mmols) and KSCN (140 mg, 1.54 mmols) in 50 mL absolute ethanol was refluxed under nitrogen for 24 h. Solvent was evaporated under vacuum and the residue extracted with 25 mL warm CH<sub>2</sub>Cl<sub>2</sub>. The yellow-orange extract was passed through a thin pad of glass wool and the filtrate was

layered with hexane. Cooling at  $-15^{\circ}\text{C}$  overnight yielded 99 mg (29%) **2b** $\bullet\text{CH}_2\text{Cl}_2$  as a yellow-orange solid. The  $\text{CH}_2\text{Cl}_2$  can be removed by gentle heating under vacuum to form **2b**. The low yield is attributed to the poor solubility of **2b** in many polar solvents including  $\text{CH}_2\text{Cl}_2$ . Polar solvents with the potential to act as Lewis bases (acetone, acetonitrile, alcohols, DMSO) were avoided to prevent possible dissociation of the thiocyanide ligand and formation of a solvated  $[\text{CpRu}(\text{PPh}_3)(\text{PPh}_2\text{Me})(\text{solvent})]^+$  cation as observed for  $\text{CpRu}(\text{PPh}_3)(\text{PPh}_2\text{Me})\text{X}$  ( $\text{X}=\text{Cl}, \text{Br}, \text{I}$ ).<sup>4</sup> M.p. decomposes without melting above  $160^{\circ}\text{C}$ . IR:  $\nu_{\text{CN}} = 2103 \text{ cm}^{-1}$ .  $^1\text{H}$  (400 MHz,  $\text{CDCl}_3$ ):  $\delta$  7.0–7.6 (m, 25H, aryl), 5.30 (s,  $\text{CH}_2\text{Cl}_2$ ), 4.35 (s, 5H, Cp), 1.07 (d,  $J = 8.4 \text{ Hz}$ , 3H,  $\text{CH}_3$ ).  $^{31}\text{P}\{{}^1\text{H}\}$  (162 MHz,  $\text{CDCl}_3$ ):  $\delta$  29.5 (d,  $J=39 \text{ Hz}$ ), 46.5 (d,  $J=39 \text{ Hz}$ ); (THF)  $\delta$  46.8 ppm (d,  $J_{\text{pp}}=41 \text{ Hz}$ ), 29.4 (d, 41 Hz). Anal. Calcd for  $\text{C}_{37}\text{H}_{33}\text{NP}_2\text{RuS}$ : C, 64.71%; H, 4.86%. Found: C, 64.31%; H, 4.20%.

Crystals of **2b** $\bullet\text{CH}_2\text{Cl}_2$  were grown by slow evaporation of a  $\text{CH}_2\text{Cl}_2$  solution but proved to be disordered limiting the quality of the crystal structure. In the opinion of two crystallographers,<sup>5</sup> the problem is a very sophisticated form of molecular disorder that is beyond all the normal treatments we use for simple atom positional disorder. The disorder prevents refinement of bond lengths and angles, but the structure showing an S-bonded thiocyanate ligand and a bent Ru–S–C bond is trustworthy (see Figure S3). Further complications arise from the loss of diffraction data in a hard drive crash at Tufts University.

#### *Synthesis of $\text{CpRu}(\text{PPh}_3)_2\text{SeCN}$ (3b)*

A slurry of  $\text{CpRu}(\text{PPh}_3)_2\text{Cl}$  (444 mg, 0.61 mmols) and KSeCN (488 mg, 3.39 mmols) in 50 mL absolute ethanol was stirred under nitrogen for 10 days. The orange slurry turned yellow over the course of the reaction. (Heating the mixture leads to black solids. Shorter reaction times tend to reduce yields.) Addition of 50 mL toluene resulted in a red-orange solution. After filtering, solvent volume was reduced under vacuum to about 20 mL. Careful addition of hexane as a separate layer and cooling to  $-20^{\circ}\text{C}$  overnight precipitated 314 mg (65%) **3b** as a red solid. The product can be chromatographed on alumina with  $\text{CH}_2\text{Cl}_2$  but a small amount of  $\text{CpRu}(\text{PPh}_3)_2\text{Cl}$  tends to form. Compound **3b** may be recrystallized from methyl(<sup>t</sup>butyl)ether/hexane however, crystals suitable for x-diffraction were grown from toluene/hexane.

M.p. 137–139°C, melts to a red-orange liquid. IR:  $\nu_{\text{CN}} = 2097 \text{ cm}^{-1}$ .  $^1\text{H}$  (400 MHz,  $\text{C}_6\text{D}_6$ ):  $\delta$  7.26 (br m, 18H, aryl), 6.58 (m, 12 H, aryl), 4.28 (s, 5H, Cp); (400 MHz,  $\text{CDCl}_3$ ):  $\delta$  7.30 (m, 18H, aryl), 7.20 (m, 12H, aryl), 4.26 (s, 5H, Cp);  $^{31}\text{P}\{{}^1\text{H}\}$  (162 MHz,  $\text{C}_6\text{D}_6$ ):  $\delta$  41.17 s; ( $\text{CDCl}_3$ ): 41.81 s; ( $\text{C}_6\text{H}_5\text{F}/10\% \text{ C}_6\text{D}_6$ )  $\delta$  40.92 (s).

#### *Synthesis of $\text{CpRu}(\text{PPh}_3)(\text{PMePh}_2)\text{SeCN}$ (4b)*

A solution of **3b** (124.5 mg, 0.157 mmols) and 30 $\mu\text{L}$  (0.16 mmol)  $\text{PMePh}_2$  in 10 mL fluorobenzene was stirred at ambient temperature for 5 days precipitating a yellow solid. After filtering and washing with pentane, 35.3 mg (31% yield) of  $\text{CpRu}(\text{PPh}_3)(\text{PMePh}_2)\text{SeCN}$  is obtained. Compound **4b** was characterized further by X-ray diffraction. Like **2b**, there is considerable disorder in the structure, with a mirror-related disorder in the phosphine ligands but the R values (Table S17,  $\text{R}_1 = 0.106$ ,  $\text{wR}_2 = 0.227$ ) are sufficient to confirm coordination through selenium and a bent Ru–Se–CN bond.

M.p. 160°C d. IR:  $\nu_{\text{CN}} = 2097 \text{ cm}^{-1}$ .  $^1\text{H}$  (400 MHz,  $\text{CDCl}_3$ ):  $\delta$  7.0-7.8 (m, 25H, aryl), 4.48 (s, 5H, Cp), 1.23 (d,  $J = 8.8 \text{ Hz}$ , 3H,  $\text{CH}_3$ ).  $^{31}\text{P}\{\text{H}\}$  (162 MHz,  $\text{CDCl}_3$ ):  $\delta$  27.74 (d,  $J=39 \text{ Hz}$ ), 46.05 (d,  $J=38 \text{ Hz}$ ); ( $\text{C}_6\text{D}_6$ )  $\delta$  46.52 (d,  $J_{\text{pp}}=38 \text{ Hz}$ ), 27.97 (d, 38 Hz); ( $\text{C}_6\text{H}_5\text{F}/10\% \text{ C}_6\text{D}_6$ ) 46.47 (d,  $J=38 \text{ Hz}$ ), 27.48 (d,  $J=38 \text{ Hz}$ ).

#### *Attempted Synthesis of $\text{CpRu}(\text{PPh}_3)_2\text{TeCN}$ (5)*

A slurry of 192.6 mg (0.31 mmol)  $\text{CpRu}(\text{PPh}_3)_2\text{Cl}$  and 225.6 mg (0.31 mmol)  $\text{PPN}\text{TeCN}$ <sup>6</sup> in 10 mL toluene was stirred at ambient temperature. No reaction was observed by  $^{31}\text{P}$  NMR and subsequent heating of the mixture produced a black intractable product.

#### *Synthesis of $^n\text{Bu}_4\text{NSeCN}$*

By analogy to the synthesis of  $\text{Me}_4\text{NSeCN}$ ,<sup>7</sup> slurry of  $^n\text{Bu}_4\text{Cl}$  (421 mg, 1.51 mmol) and  $\text{KSeCN}$  (221 mg, 1.54 mmol) in 20 mL fluorobenzene was stirred for 7 days at ambient temperature for 7 days. After filtering to remove  $\text{KCl}$ , solvent was evaporated from the filtrate yielding a sticky white solid which solidified upon standing, yielding 314 mg (61 % yield) of  $^n\text{Bu}_4\text{NSeCN}$ . M.p. 139-141.5 °C melts to a colorless liquid.  $^1\text{H}$  (400 MHz,  $\text{CDCl}_3$ ):  $\delta$  1.03 (t, 3H), 1.48 (m, 2H), 1.70 (m, 2H), 3.32 (m, 2 H).  $^{13}\text{C}\{\text{H}\}$  (100.63 MHz,  $\text{CDCl}_3$ ):  $\delta$  13.69, 19.80, 24.13, 59.05, 117.36.

#### *Kinetic Measurements*

Kinetic data for reactions between **1a** or **3b** and  $\text{PMcPh}_2$  is collected using procedures described for reactions between  $\text{CpRu}(\text{PAr}_3)_2\text{Cl}$  and  $\text{PMcPh}_2$ .<sup>8</sup> Flame-sealed 5 mm NMR tubes containing solutions of **1a** or **3b** (5-7 mM) and  $\text{PMcPh}_2$  ( $\approx$  50-70 mM) in THF/10% (v/v)  $\text{C}_6\text{D}_6$  or  $\text{C}_6\text{H}_5\text{F}/10\% \text{ C}_6\text{D}_6$  are heated in thermostated block heaters. The rate of substitution of  $\text{PPh}_3$  by  $\text{PMcPh}_2$  is measured by monitoring the decrease in the singlet for **1a** or **3b** over time relative to the doublets for  $\text{CpRu}(\text{PPh}_3)(\text{PMcPh}_2)\text{NCS}$  (**2a**) and  $\text{CpRu}(\text{PPh}_3)(\text{PMcPh}_2)\text{SeCN}$  (**4b**). Typically, three independent measurements of the substitution rate are made at each temperature to determine the rate constants for the reaction.

The reactions were typically driven to  $\geq 80\%$  completion for three reasons. First, beyond 90% reaction signal-to-noise ratio for the lowest intensity resonances makes it difficult to obtain accurate peak areas through integration of the resonances using reasonable scan times. Second, in the later stages of the reaction, sufficient  $\text{PPh}_3$  has built up in the reaction mixture to inhibit substitution and decrease the rate of phosphine exchange. The result is a curvature in the plot of  $\ln[\mathbf{1a}]$  (or  $\ln[\mathbf{3b}]$ ) vs time. Finally, for reactions of **1a** at lower temperatures (e. g 40°C), the reactions are quite slow ( $> 14$  days) so in these cases, data collection was ended after reaching 80% completion.

#### **Computational Methods**

All computations were run on the Northeastern University Discovery Cluster. We report the Cartesian coordinates of all the structures optimized using Kohn-Sham density functional theory (M06).

The gas phase calculations on **1-4** were completed over five years ago and relied on the available computational packages found in GaussView 3 and Gaussian 09 Revision B.01 suite.<sup>9</sup> Geometries were optimized followed by harmonic frequency analysis to obtain free energy corrections for each compound. The geometry optimizations and

frequency calculations were performed using the unrestricted UB3LYP exchange-correlation. Each compound was optimized and analyzed twice using two different basis sets. The DGDZVP<sup>10</sup> and LANL2DZ<sup>11</sup> basis sets were used to perform the calculations. Both basis sets are of double-zeta quality in the valence shell. First an optimization for a compound was run followed by a harmonic frequency analysis using the same basis set. Optimized geometries were visualized using Avogadro (V 1.1.1).<sup>12</sup> Spin multiplicity was assumed to be 1 and overall charge was assumed to be 0. The following was used in the route section for all compounds:

```
# opt freq scf=(maxcycle=1024) ub3lyp/basis pop=full
```

where basis refers to the basis used in the calculation, either DGDZVP or LANL2DZ.

The calculations for **1-4** as benzene solvates used the updated Gaussian16 Revision A.03 suite of ab initio quantum chemistry programs using the M06 functional, the def2-TZVP basis set, Grimme's D3 dispersion correction and the Polarizable Continuum Model (PCM) provided by Gaussian.<sup>13</sup>

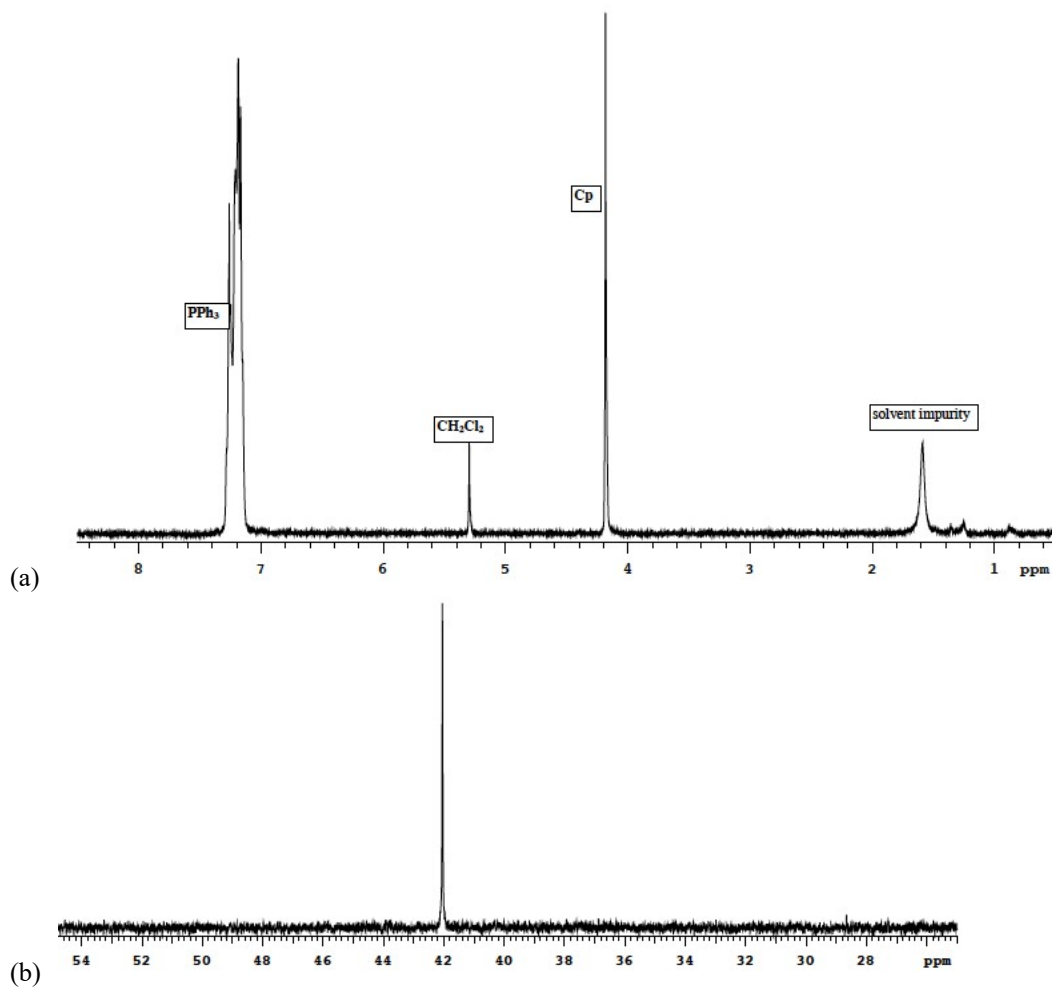


**Figure S1:** (a)  $^1\text{H}$  NMR spectrum of **1a** in  $\text{CDCl}_3$ ; (b)  $^{31}\text{P}$  NMR spectrum of **1a** in  $\text{CDCl}_3$ .

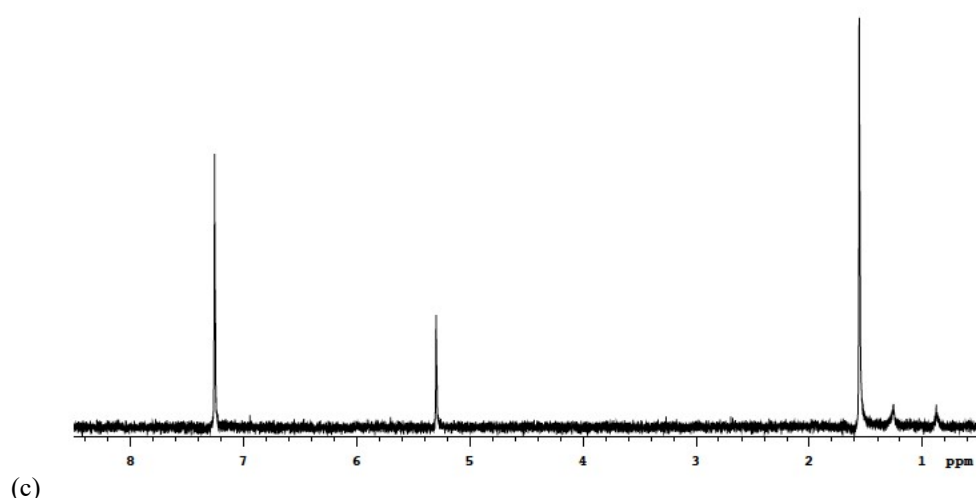
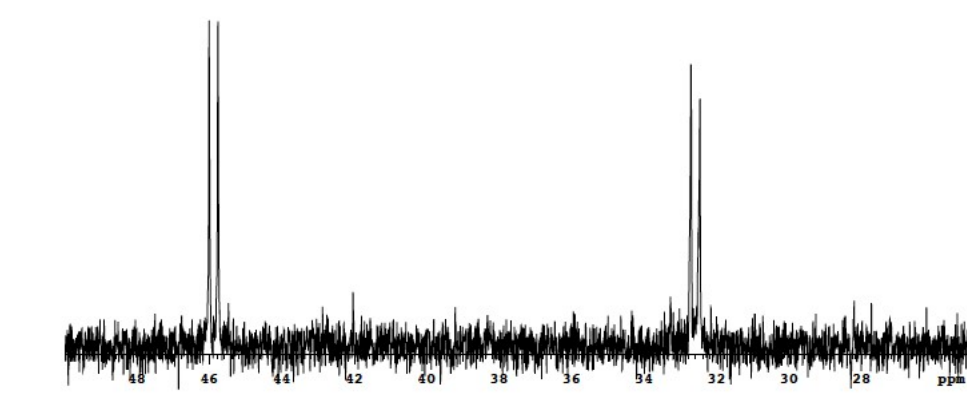
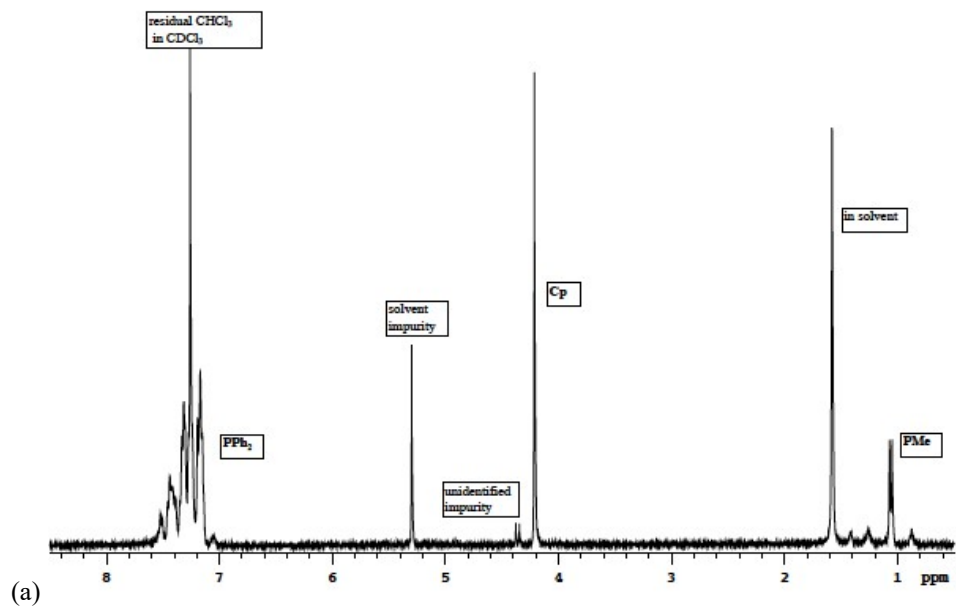


**Figure S2:** (a) <sup>1</sup>H NMR spectrum of **2a** ( $\text{CH}_2\text{Cl}_2$  often co-crystallizes); (b) <sup>31</sup>P NMR spectrum of **2a**; (c) <sup>1</sup>H NMR spectrum of  $\text{CDCl}_3$

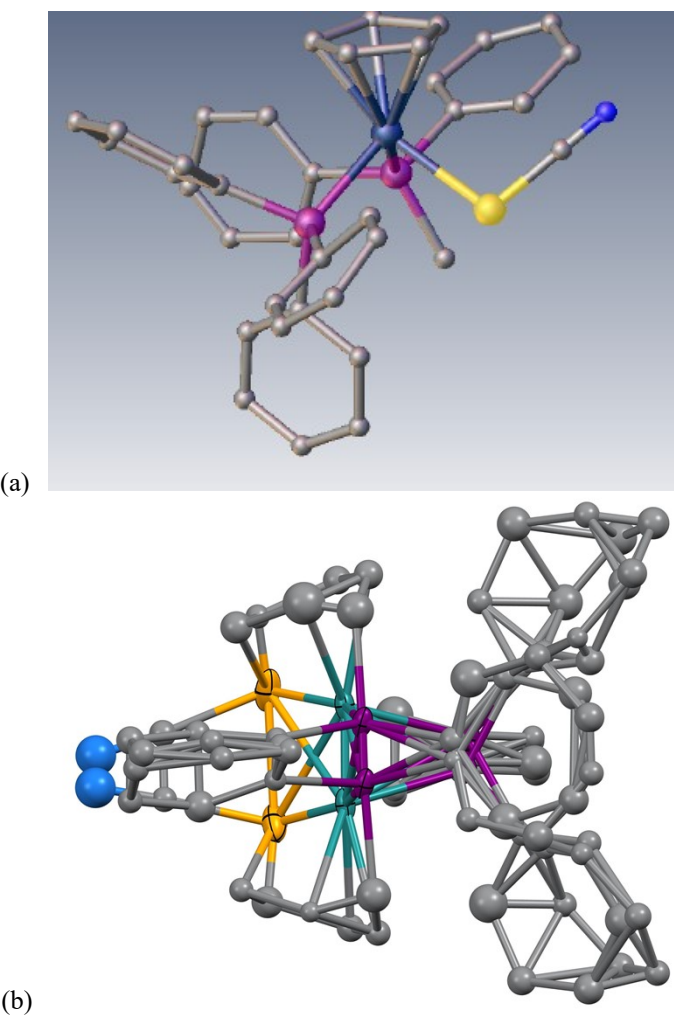


**Figure S3:** (a) Best molecular structure of **2b** based on molecular disorder that is beyond all the normal treatments we use for simple atom positional disorder. (b) Two superimposed orientations of **4b** showing the mirror-related disorder in the structure.

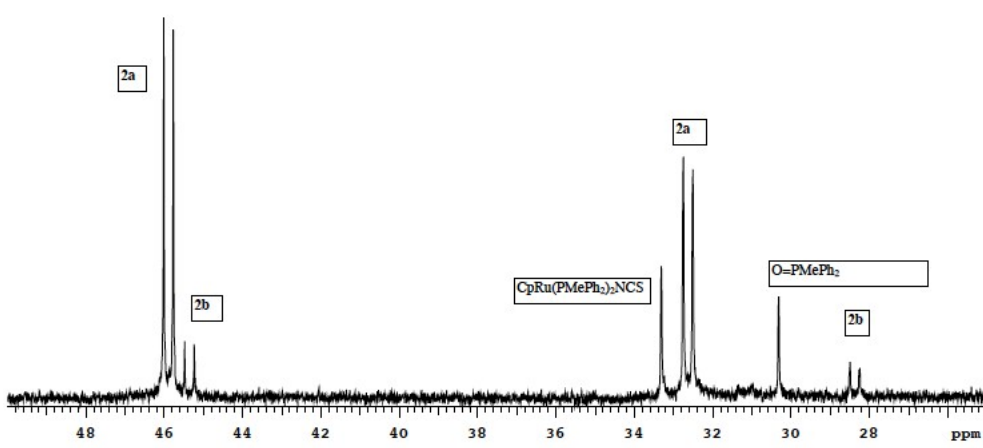
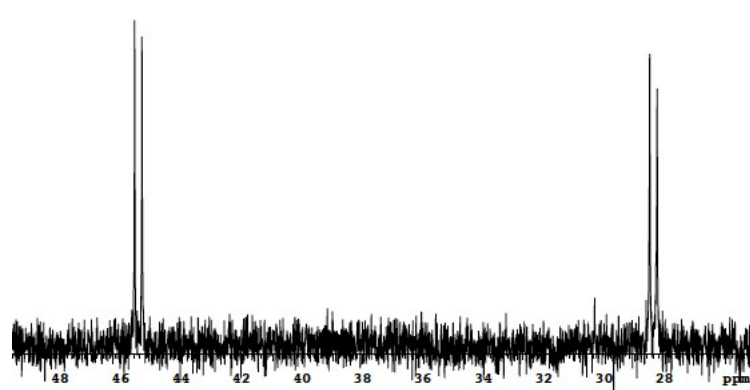
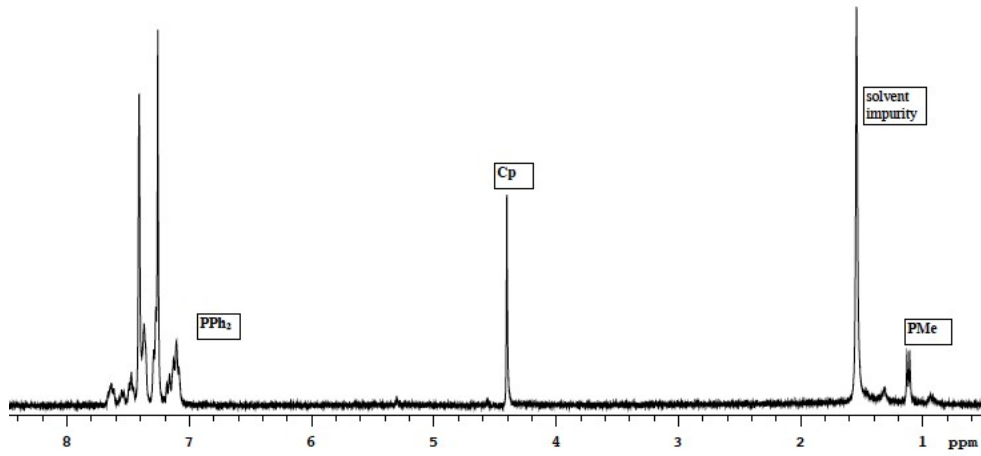


**Figure S4:** (a)  $^1\text{H}$  NMR spectrum of dilute solution of **2b** in  $\text{CDCl}_3$ ; (b)  $^{31}\text{P}$  NMR spectrum of **2b** in  $\text{CDCl}_3$ ; (c)  $^{31}\text{P}$  NMR of a mixture of **2a** and **2b** in  $\text{CDCl}_3$  prior to re-crystallization to remove the two impurities shown in the spectrum.

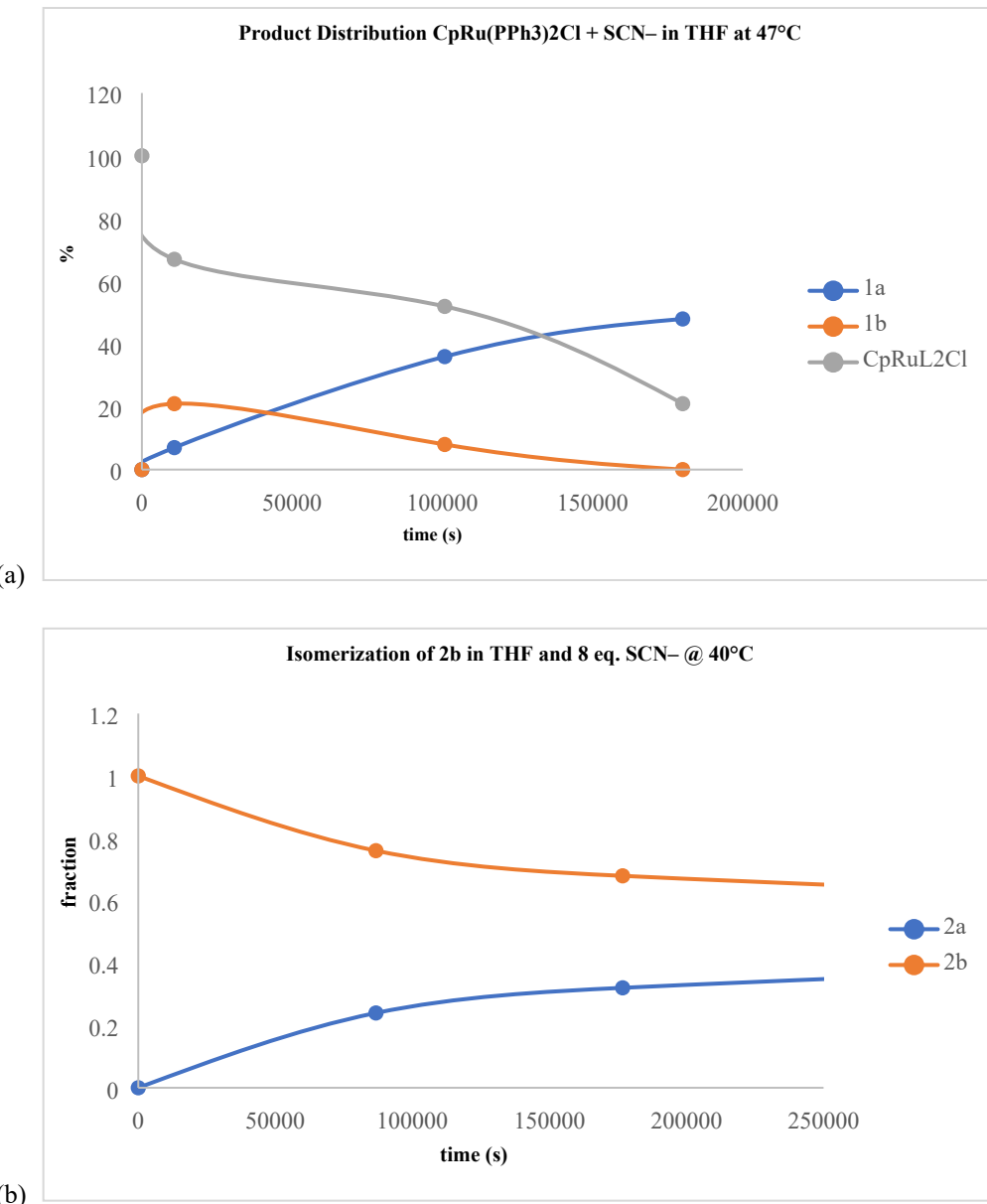


**Figure S5:** (a) Reaction of CpRu(PPh<sub>3</sub>)<sub>2</sub>Cl with SCN<sup>-</sup> in THF @ 47°C (b) isomerization of **2b** to **2a** with SCN<sup>-</sup> in THF/10% C<sub>6</sub>D<sub>6</sub> @ 40°C

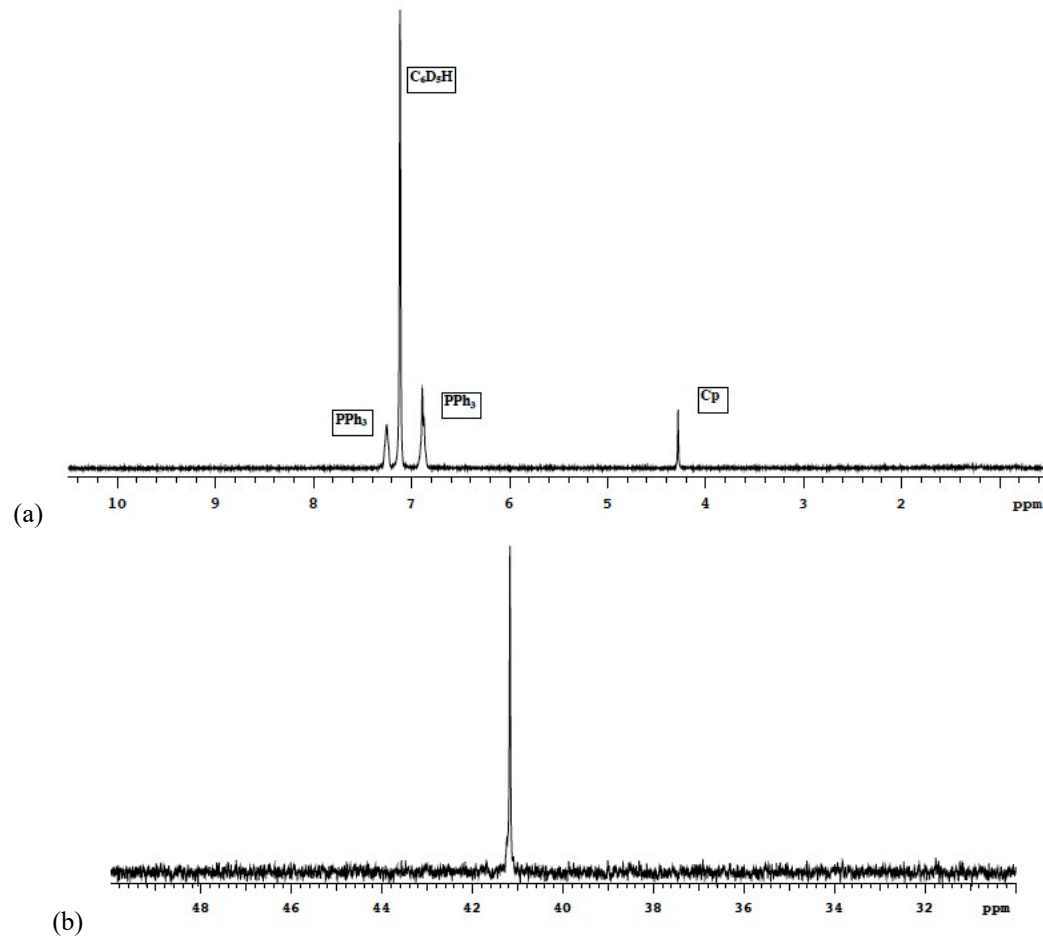


**Figure S6:** (a)  $^1H$  NMR spectrum of **3b** in  $C_6D_6$ ; (b)  $^{31}P$  NMR spectrum of **3b** in  $C_6D_6$ .

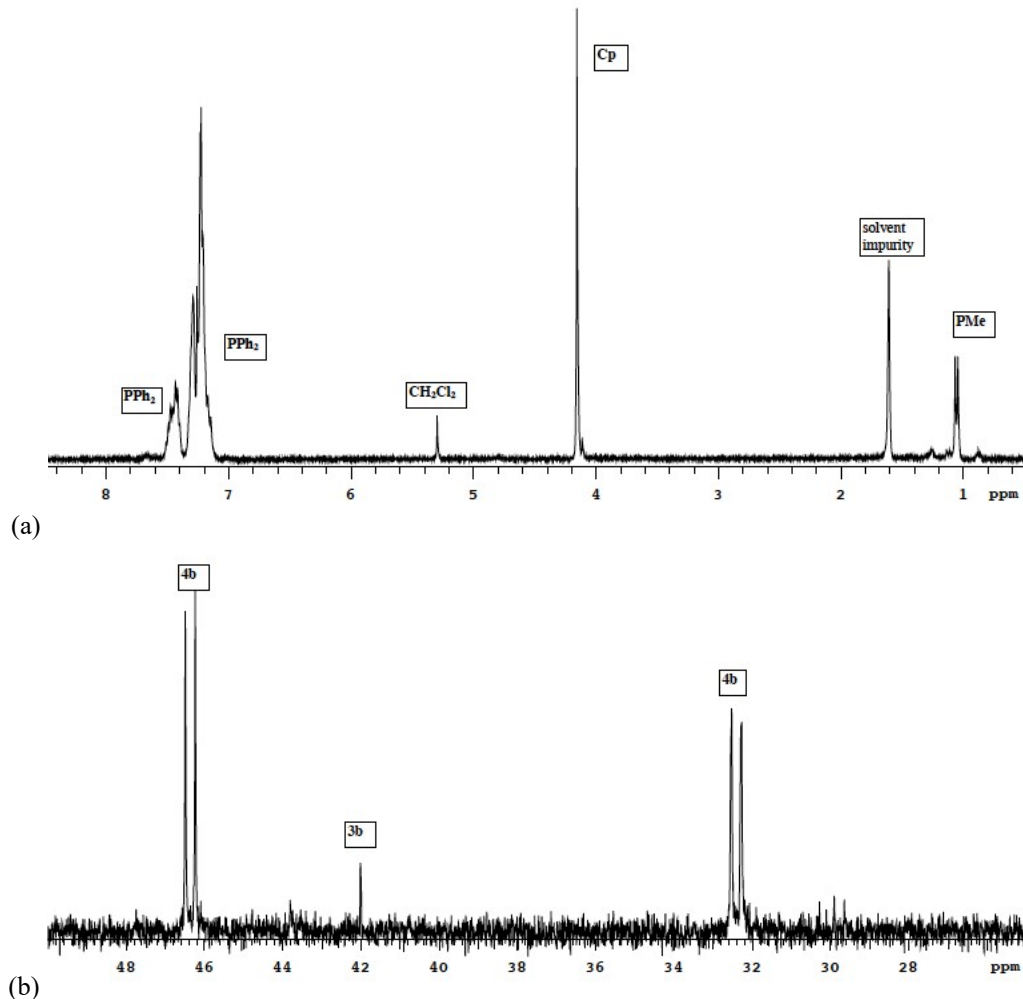


**Figure S7:** (a)  $^1\text{H}$  NMR spectrum of **4b** in  $\text{CDCl}_3$  (some  $\text{CH}_2\text{Cl}_2$  often retained by crystalline products); (b)  $^{31}\text{P}$  NMR spectrum of **4b** in  $\text{CDCl}_3$  ( $\approx 4\%$  impurity of **3b**).

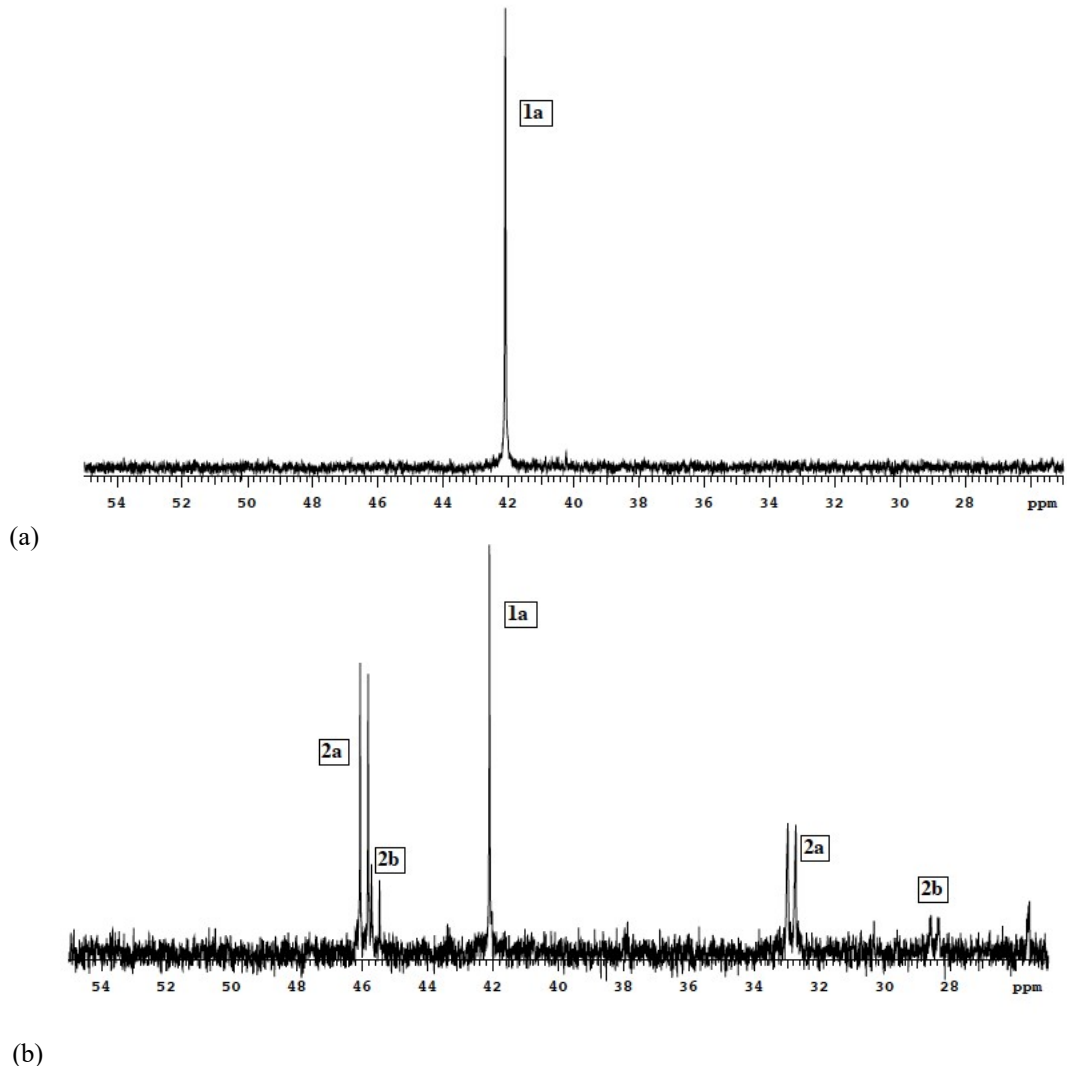


**Figure S8:** (a)  $^{31}\text{P}$  NMR spectrum of **1a** (5 mM) + PMePh<sub>2</sub> (41 mM) in C<sub>6</sub>H<sub>5</sub>F/10% v/v C<sub>6</sub>D<sub>6</sub> at t=0 s; (b)  $^{31}\text{P}$  NMR spectrum of **1a** + PMePh<sub>2</sub> in C<sub>6</sub>H<sub>5</sub>F/10% v/v C<sub>6</sub>D<sub>6</sub> after heating at 40°C for 317 h showing 76% conversion to **2a** with small amounts of **2b**. Resonances for PPh<sub>3</sub> (−5.33 ppm) and PMePh<sub>2</sub> (−27.26 ppm) are not shown.

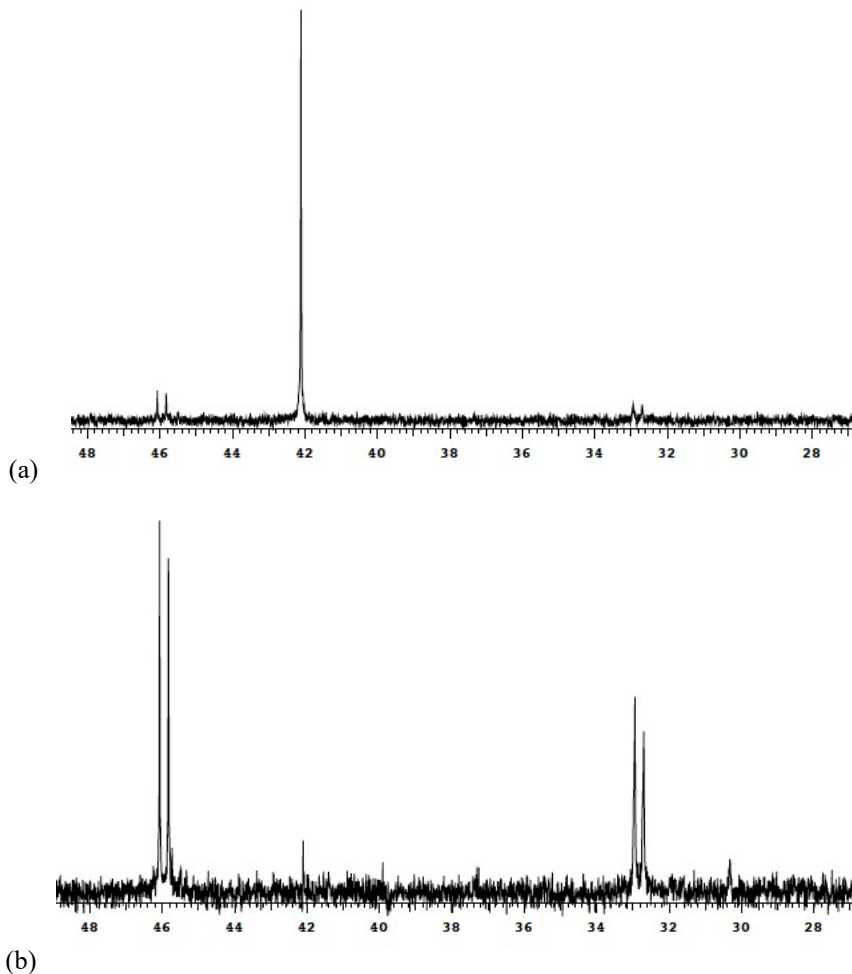


**Figure S9:** (a)  $^{31}\text{P}$  NMR spectrum of **1a** (5 mM) + PMePh<sub>2</sub> (39 mM) in C<sub>6</sub>H<sub>5</sub>F/10% v/v C<sub>6</sub>D<sub>6</sub> after heating at 50°C for 21.5 h; (b)  $^{31}\text{P}$  NMR spectrum of **1a** + PMePh<sub>2</sub> in C<sub>6</sub>H<sub>5</sub>F/10% v/v C<sub>6</sub>D<sub>6</sub> after heating at 50°C for 150 h showing 96% conversion to **2a**. Resonances for PPh<sub>3</sub> (−5.33 ppm) and PMePh<sub>2</sub> (−27.26 ppm) are not shown.

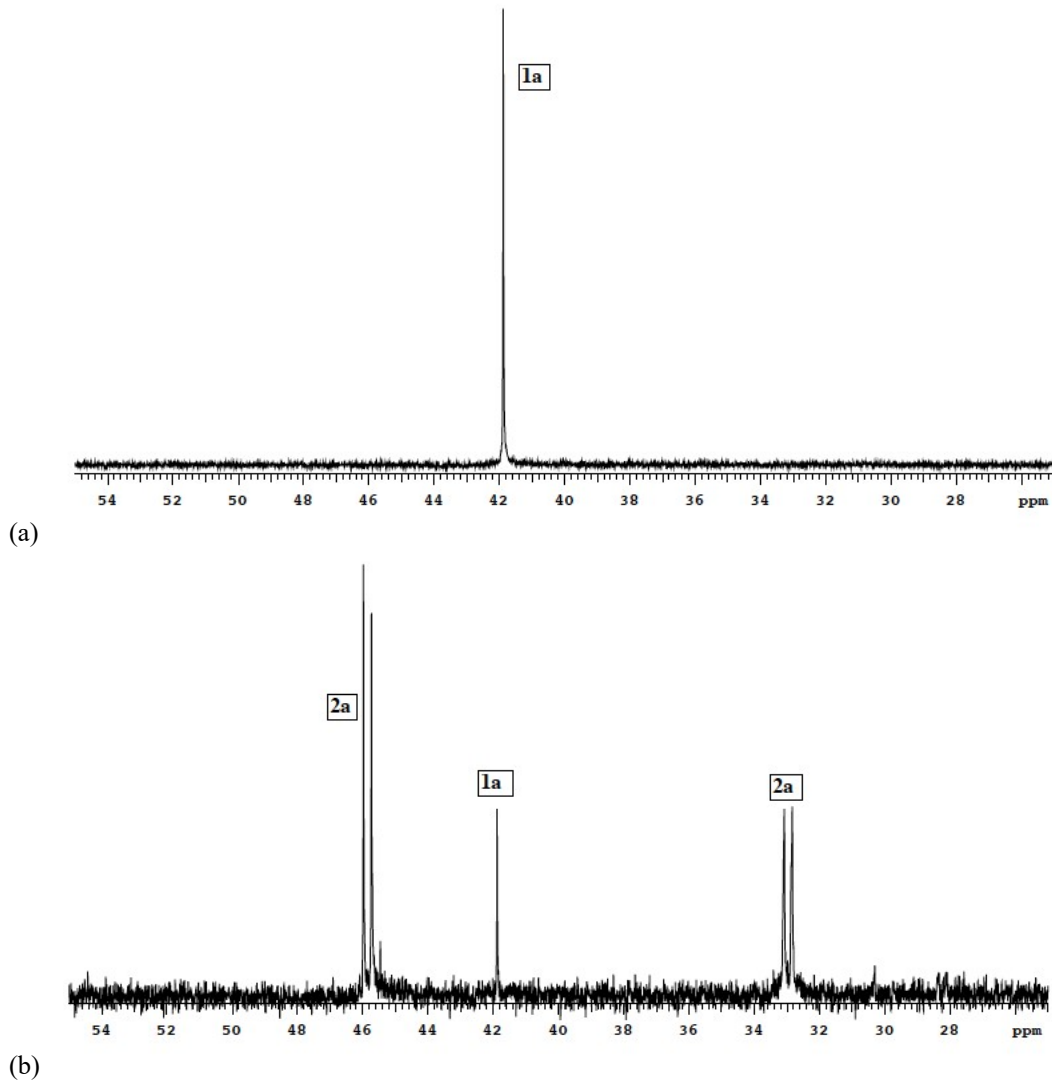


**Figure S10:** (a)  $^{31}\text{P}$  NMR spectrum of **1a** (5 mM,  $^{31}\text{P}$ :  $\delta$  42 ppm) +  $\text{PMePh}_2$  (41 mM) in  $\text{THF}/10\% \text{ v/v C}_6\text{D}_6$  at  $t=0$  s; (b)  $^{31}\text{P}$  NMR spectrum of **1a** +  $\text{PMePh}_2$  in  $\text{THF}/10\% \text{ v/v C}_6\text{D}_6$  after heating at  $40^\circ\text{C}$  for 317 h showing 93% conversion to **2a**. Resonances for  $\text{PPh}_3$  ( $-5.86$  ppm) and  $\text{PMePh}_2$  ( $-27.46$  ppm) are not shown.

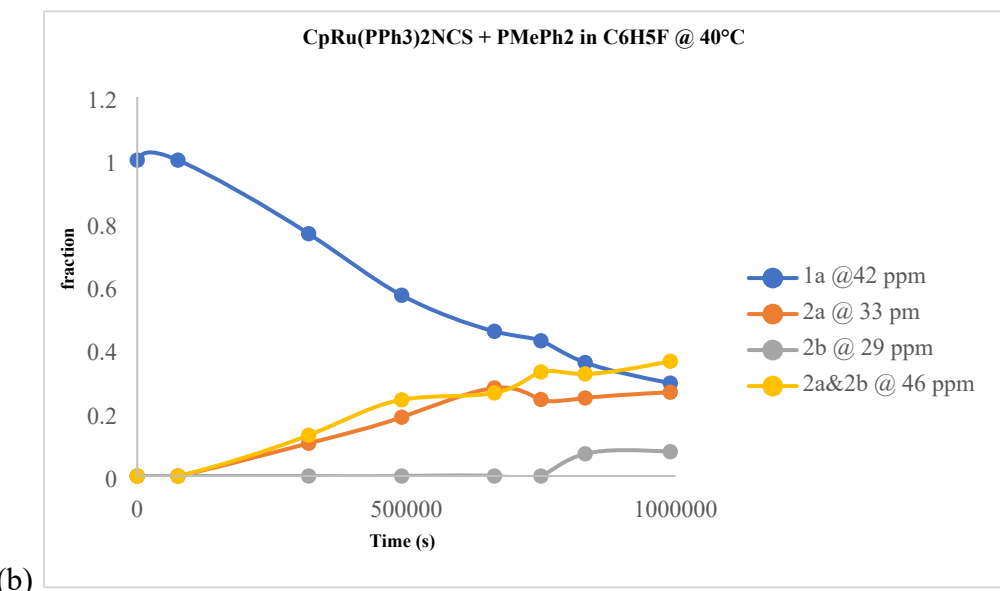
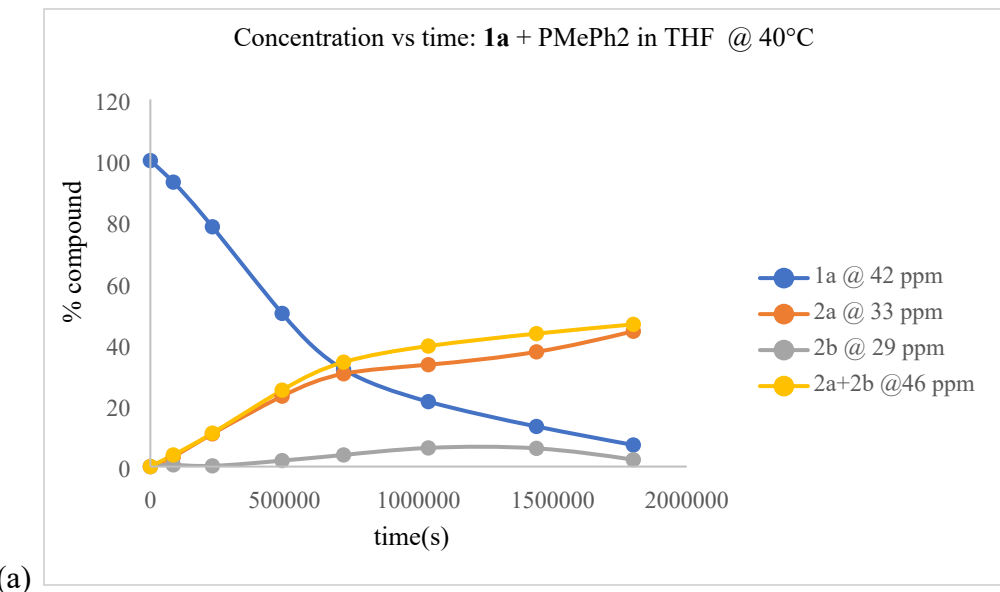


**Figure S11:** Concentration Changes in the Reaction Between **1a** and PMePh<sub>2</sub> @ 40°C in (a) THF/10% C<sub>6</sub>D<sub>6</sub> @ 40°C and (b) C<sub>6</sub>H<sub>5</sub>F/10% C<sub>6</sub>D<sub>6</sub>.

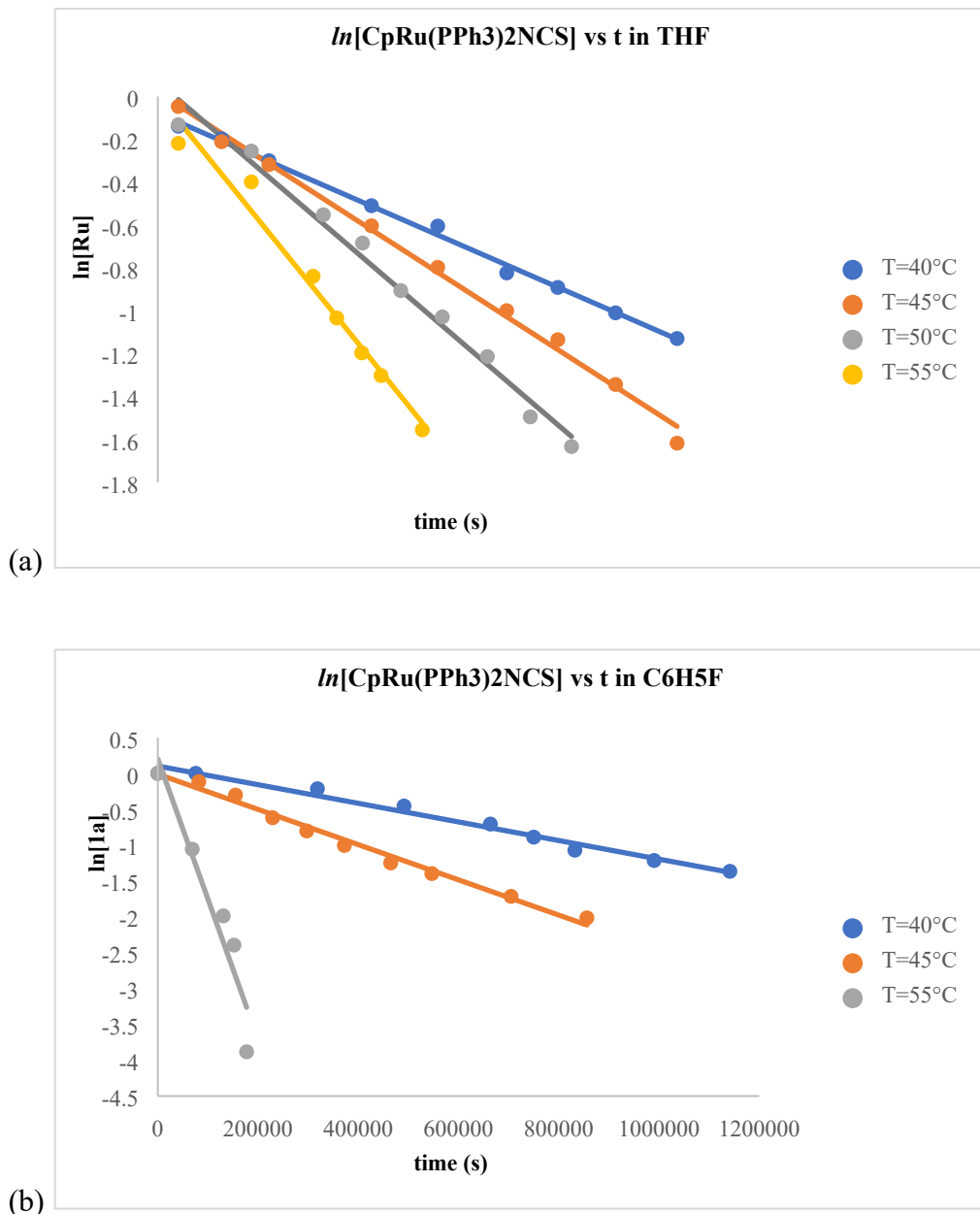


**Figure S12:** Representative plots of  $\ln[\text{CpRu}(\text{PPh}_3)_2\text{NCS}]$  vs  $t$  for the reaction between **1a** and  $\text{PMePh}_2$  in (a) THF/10%  $\text{C}_6\text{D}_6$  and (b)  $\text{C}_6\text{H}_5\text{F}/10\%$   $\text{C}_6\text{D}_6$

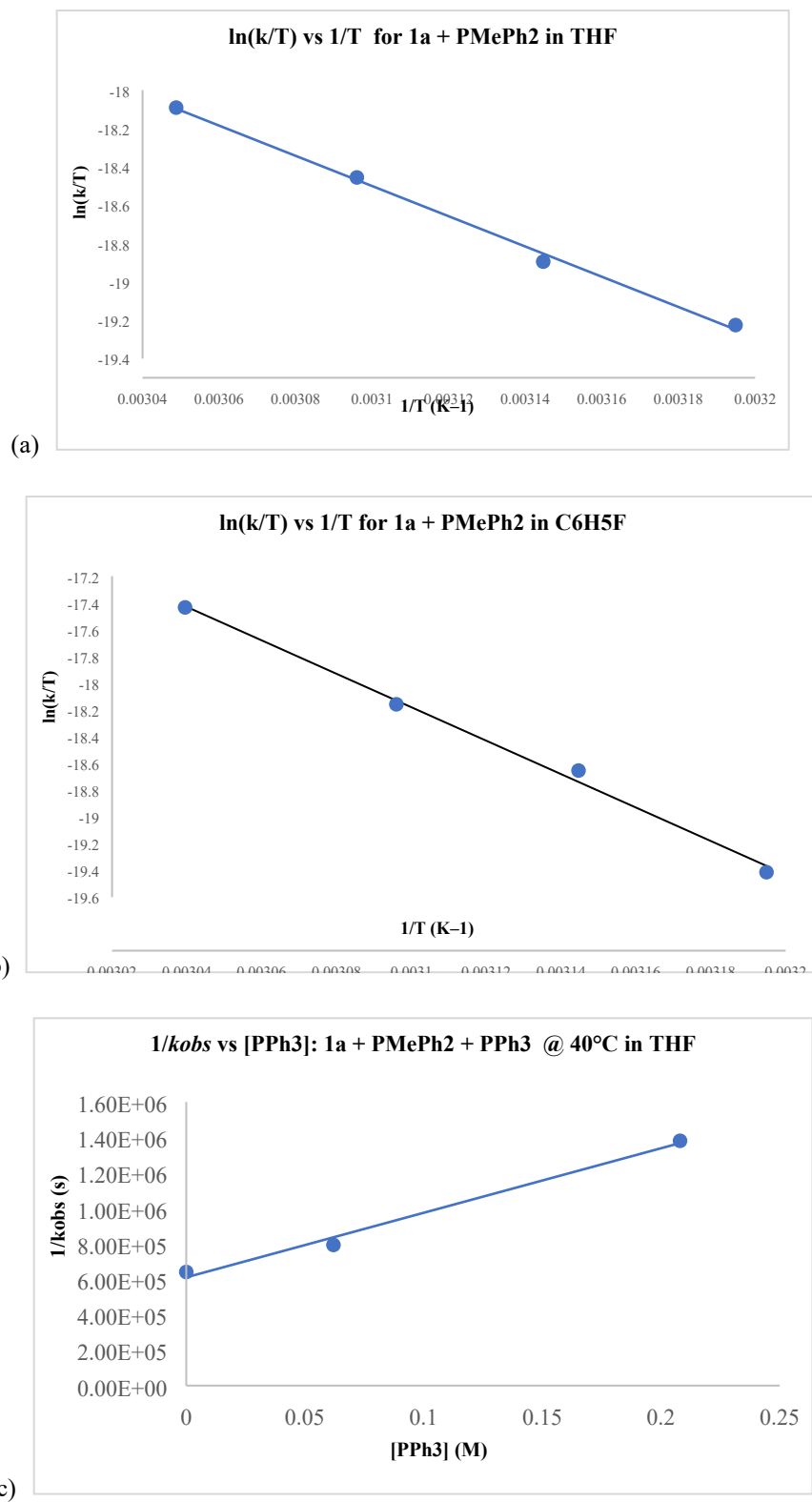


**Figure S13:** Eyring plots for the reaction between **1a** and PMePh<sub>2</sub> (a) in THF/10% C<sub>6</sub>D<sub>6</sub>; (b) in C<sub>6</sub>H<sub>5</sub>F/10% C<sub>6</sub>D<sub>6</sub> and (c) Plot of 1/ $k_{obs}$  vs [PPh<sub>3</sub>] at 40°C in THF/10% C<sub>6</sub>D<sub>6</sub>.

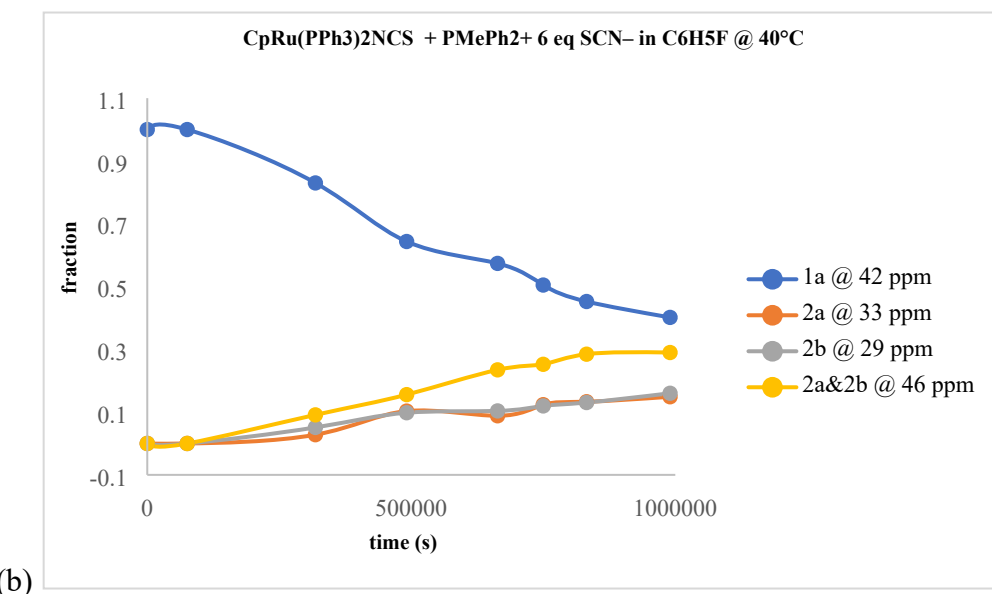
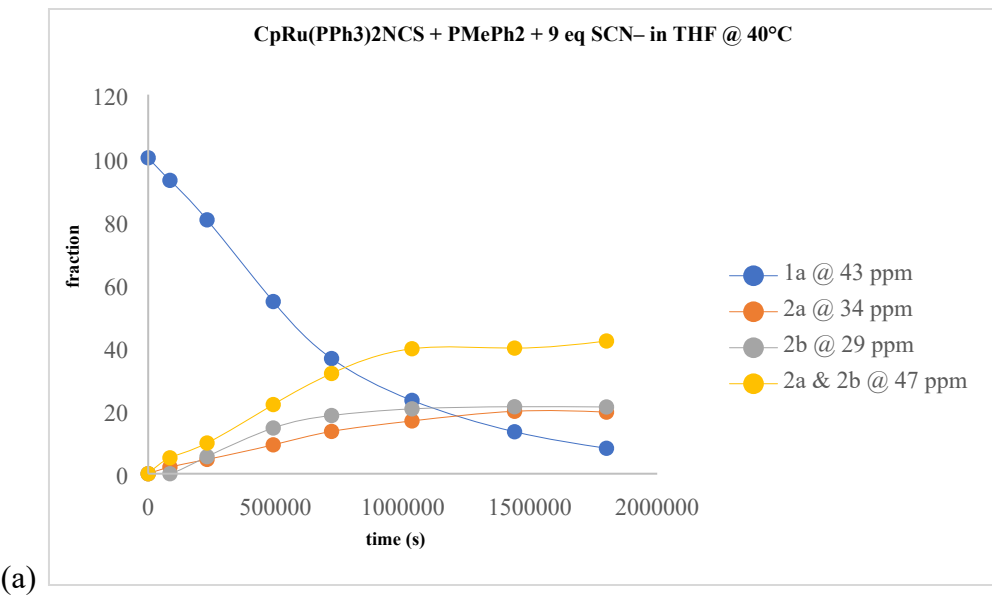
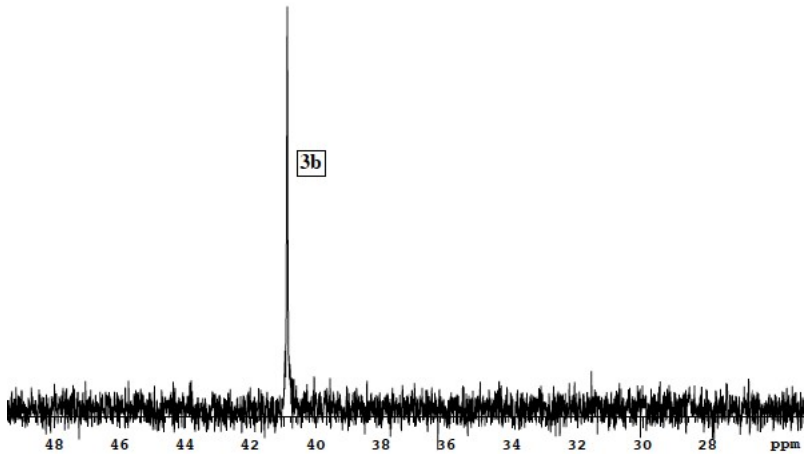


**Figure S14:** Concentration Changes in the Reaction Between **1a**, PMePh<sub>2</sub>, and SCN<sup>-</sup> @ 40°C in (a) THF/10% C<sub>6</sub>D<sub>6</sub> and (b) in C<sub>6</sub>H<sub>5</sub>F/10% C<sub>6</sub>D<sub>6</sub>.



(a)

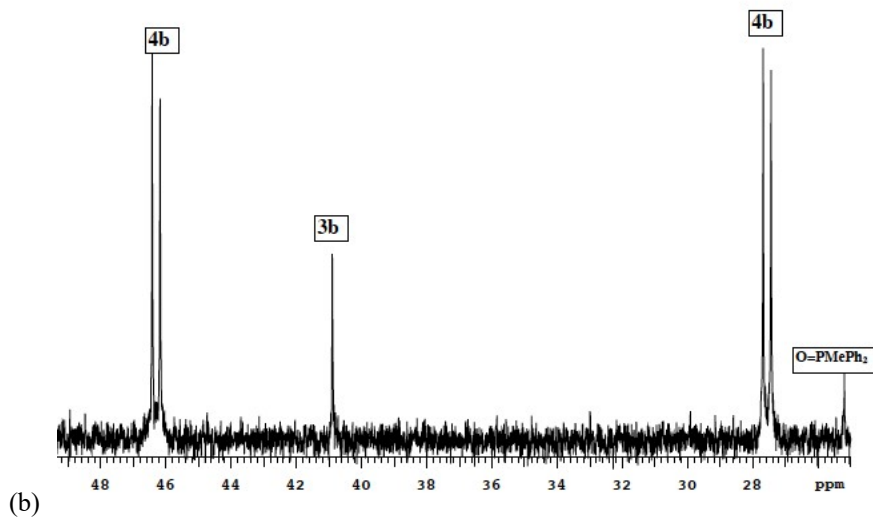


**Figure S15:** (a)  ${}^3\text{P}$  NMR spectrum of **3b** (5.7 mM) + PMePh<sub>2</sub> (50 mM) in C<sub>6</sub>H<sub>5</sub>F/10% v/v C<sub>6</sub>D<sub>6</sub> at t=0; (b)  ${}^3\text{P}$  NMR spectrum of **3b** + PMePh<sub>2</sub> in C<sub>6</sub>H<sub>5</sub>F/10% v/v C<sub>6</sub>D<sub>6</sub> after heating at 30°C for 37.7 h showing 90% conversion to **4b**.

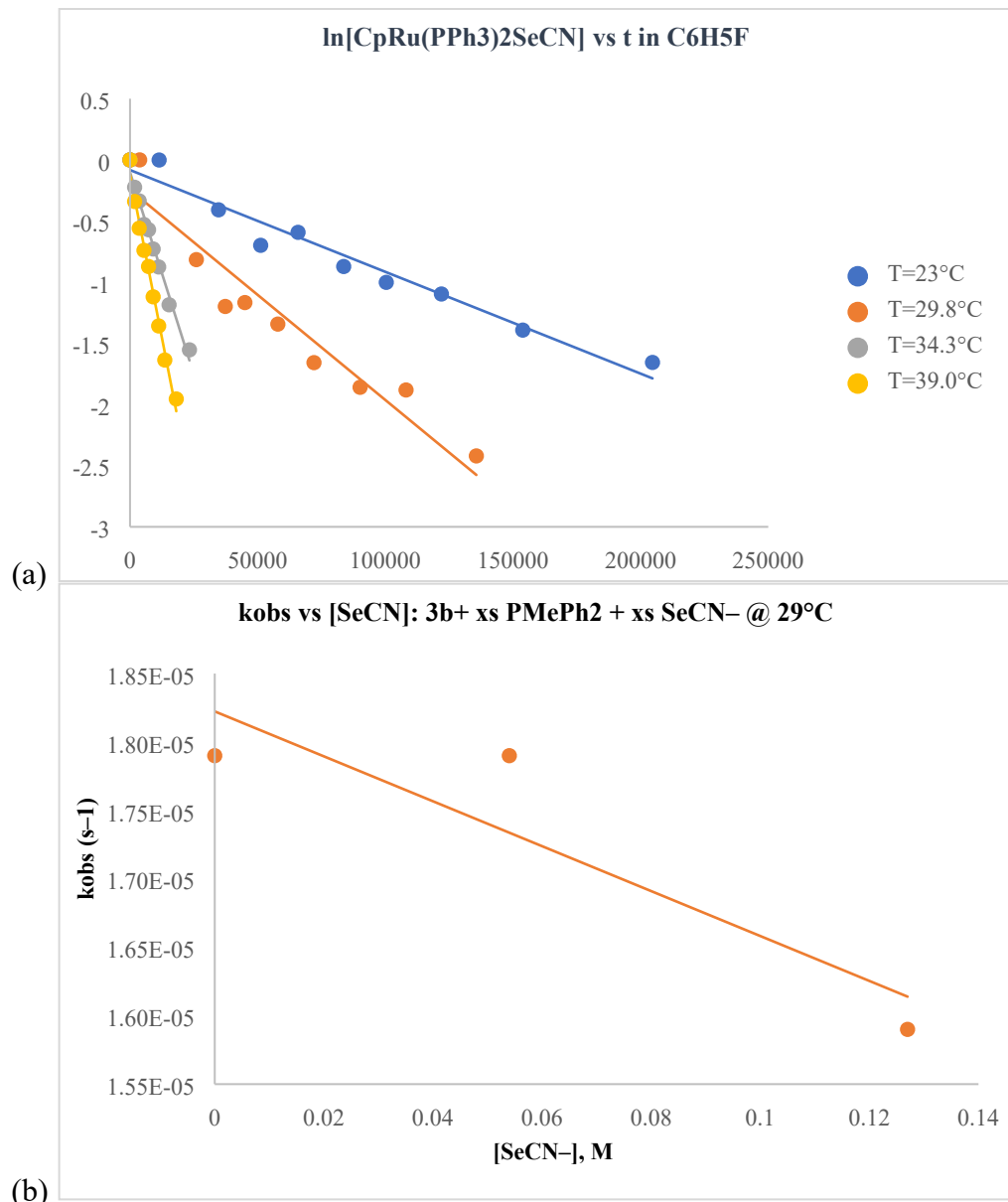


**Figure S16:** Representative plots of (a)  $\ln[\text{CpRu}(\text{PPh}_3)_2\text{SeCN}]$  vs  $t$  for the reaction between **3b** and  $\text{PMePh}_2$  in  $\text{C}_6\text{H}_5\text{F}/10\% \text{C}_6\text{D}_6$  and (b)  $k_{\text{obs}}$  vs  $[\text{SeCN}]$  @  $29^\circ\text{C}$

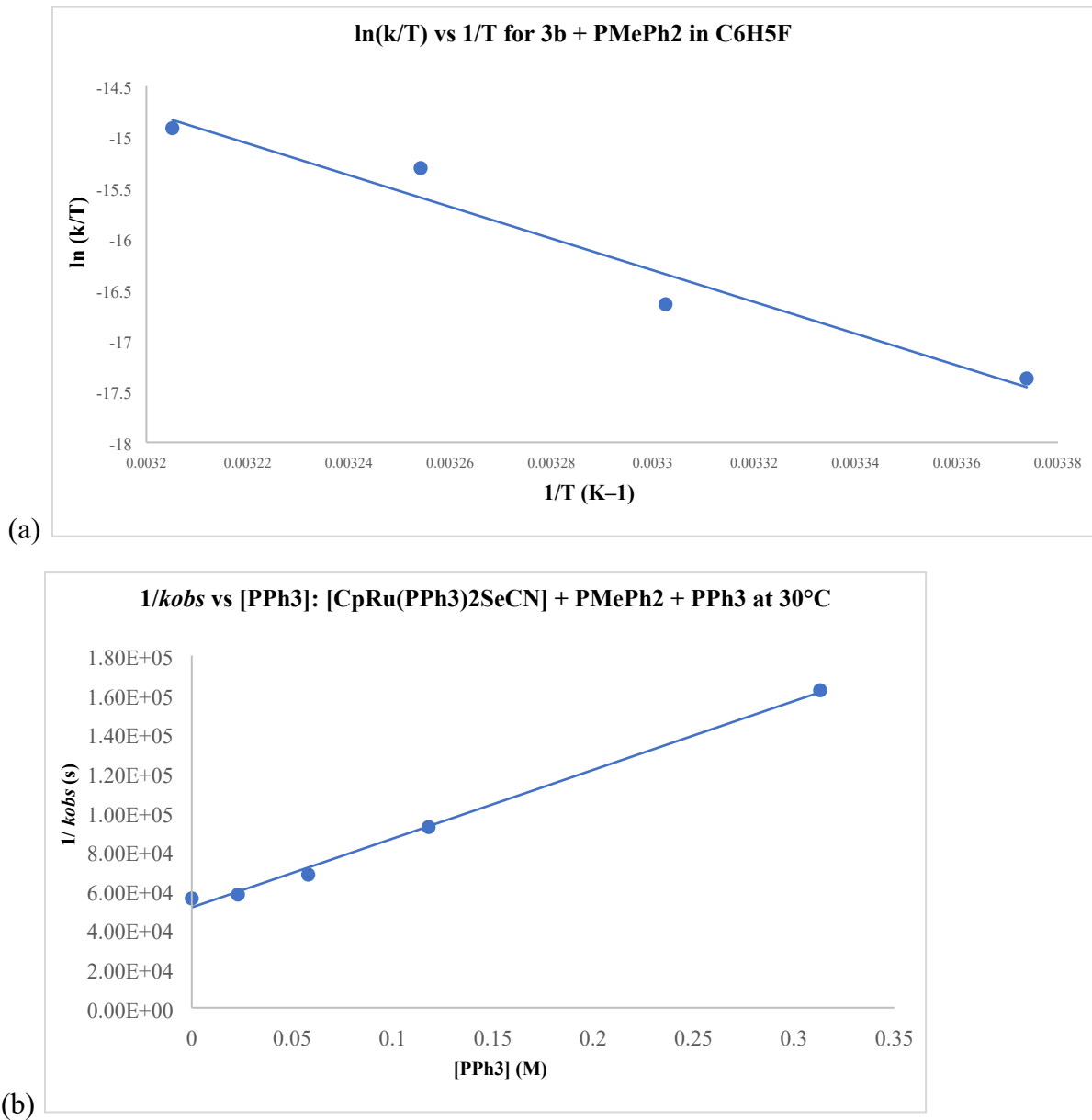


**Figure S17:** (a) Eyring plots for the reaction between **3b** and PMePh<sub>2</sub> in C<sub>6</sub>H<sub>5</sub>F/10% C<sub>6</sub>D<sub>6</sub> and (b) Plot of 1/k<sub>obs</sub> vs [PPh<sub>3</sub>]

**Table S1:** Concentrations of reactants and products: CpRu(PPh<sub>3</sub>)<sub>2</sub>NCS (**1a**) + PMePh<sub>2</sub> in THF/C<sub>6</sub>D<sub>6</sub> @ 40°C (see Figure S10 for plots)

<b>Table S1a:</b> CpRu(PPh <sub>3</sub> ) <sub>2</sub> NCS ( <b>1a</b> ) + PMePh <sub>2</sub> in THF/C <sub>6</sub> D <sub>6</sub> @ 40°C					
t (s)	δ 46 ( <b>2a&amp;2b</b> )	δ 42 ( <b>1a</b> )	δ 33 ( <b>2a</b> )	δ 29 ( <b>2b</b> )	total
0	0	100	0	0	100
85440	3.8	92.96	3.24	0.56	100
231240	10.94	78.36	10.7	0.24	100
491280	24.97	50.06	23.01	1.96	100
720480	34.13	31.75	30.33	3.80	100
1036440	39.39	21.22	33.30	6.09	100
1439520	43.45	13.11	37.49	5.95	100
1800720	46.47	7.06	44.23	2.25	100

<b>Table S1b:</b> CpRu(PPh <sub>3</sub> ) <sub>2</sub> NCS ( <b>1a</b> ) + PMePh <sub>2</sub> + 9 eq SCN <sup>-</sup> in THF/C <sub>6</sub> D <sub>6</sub> @ 40°C					
t (s)	δ 46 ( <b>2a&amp;2b</b> )	δ 42 ( <b>1a</b> )	δ 33 ( <b>2a</b> )	δ 29 ( <b>2b</b> )	total
0	0	100	0	0	100
85440	5.03	92.86	2.11	0	100
231240	9.72	80.36	4.53	5.4	100
491280	21.89	54.5	9.14	14.47	100
720480	31.73	36.46	13.39	18.42	100
1036440	39.56	23.21	16.71	20.53	100
1439520	42.30	14.13	21.02	22.55	100
1800720	46.33	8.88	21.49	23.30	100

<b>Table S1c:</b> CpRu(PPh <sub>3</sub> ) <sub>2</sub> NCS ( <b>1a</b> ) + PMePh <sub>2</sub> + 21 eq SCN <sup>-</sup> in THF/C <sub>6</sub> D <sub>6</sub> @ 40°C					
t (s)	δ 46 ( <b>2a&amp;2b</b> )	δ 42 ( <b>1a</b> )	δ 33 ( <b>2a</b> )	δ 29 ( <b>2b</b> )	total
85440	0	100	0	0	100
231240	13.53	76.32	3.22	6.93	100
491280	23.53	53.31	8.52	14.64	100
720480	29.86	38.13	9.58	22.43	100
1036440	37.38	27.24	12.83	22.55	100
1439520	41.80	16.83	14.88	26.50	100
1800720	44.50	10.86	17.37	27.27	100

**Table S2:** Rate Constants for the Reaction Between **1a** and PMe<sub>2</sub>Ph in THF containing 10% C<sub>6</sub>D<sub>6</sub>

T (°C)	[ <b>1a</b> ] (mM)	[PMePh <sub>2</sub> ] (mM)	[PPh <sub>3</sub> ] (mM)	[SCN <sup>-</sup> ] (mM)	k <sub>obs</sub> (s <sup>-1</sup> x 10 <sup>6</sup> )
40	8	128	0	0	1.35±0.24
45	8	128	0	0	2.00±0.07
50	8	128	0	0	3.14±0.09
55	8	128	0	0	4.56±0.40
40	7	76	0	0	1.56
40	7	321	0	0	1.59
40	7	76	62	0	1.22
40	7	76	208	0	0.724
40	7	76	0	64	1.41
40	7	76	0	150	1.40

**Table S3:** Rate Constants for the Reaction Between **3b** and PMe<sub>2</sub>Ph in C<sub>6</sub>H<sub>5</sub>F containing 10% C<sub>6</sub>D<sub>6</sub>

T (°C)	[ <b>3b</b> ] (mM)	[PMePh <sub>2</sub> ] (mM)	[PPh <sub>3</sub> ] (mM)	[SeCN <sup>-</sup> ] (mM)	k <sub>obs</sub> (s <sup>-1</sup> x 10 <sup>6</sup> )
23.4	5.7	50	0	0	8.45±0.3
29.8	5.7	50	0	0	17.9±0.4
34.3	5.7	50	0	0	69.2±6
39.0	5.7	50	0	0	104±4
29.8	5.7	50	23	0	17.3
29.8	5.7	50	58	0	14.7
29.8	5.7	50	118	0	10.8
29.8	5.7	50	313	0	6.16
29.8	5.7	50	0	54	17.9
29.8	5.7	50	0	127	15.9

**Table S4. Sample and crystal data for 1a.**

<b>Identification code</b>	RK1_83_a, CCDC 2282637	
<b>Chemical formula</b>	$C_{42}H_{35}NP_2RuS \bullet CH_2Cl_2$	
<b>Formula weight</b>	833.71 g/mol	
<b>Temperature</b>	100(2) K	
<b>Wavelength</b>	0.71073 Å	
<b>Crystal size</b>	0.200 x 0.200 x 0.150 mm	
<b>Crystal habit</b>	Intense yellow block	
<b>Crystal system</b>	orthorhombic	
<b>Space group</b>	Pna2 <sub>1</sub>	
<b>Unit cell dimensions</b>	a = 20.3288(10) Å	α = 90°
	b = 20.6729(10) Å	β = 90°
	c = 8.8263(4) Å	γ = 90°
<b>Volume</b>	3709.3 Å <sup>3</sup>	
<b>Z</b>	4	
<b>Density (calculated)</b>	1.493 g/cm <sup>3</sup>	
<b>Absorption coefficient</b>	0.742 mm <sup>-1</sup>	
<b>F(000)</b>	1704	

**Table S5. Data collection and structure refinement for 1a.**

<b>Theta range for data collection</b>	2.811 to 25.405°	
<b>Index ranges</b>	-24<=h<=24, -24<=k<=24, -10<=l<=10	
<b>Reflections collected</b>	9555	
<b>Independent reflections</b>	6820 [R(int) = 0.0682]	
<b>Coverage of independent reflections</b>	99.7%	
<b>Absorption correction</b>	Multi-Scan	
<b>Max. and min. transmission</b>	0.866 and 0.897	
<b>Structure solution technique</b>	direct methods	
<b>Structure solution program</b>	SHELXL-2018/2 (Sheldrick, 2018)	
<b>Refinement method</b>	Full-matrix least-squares on F <sup>2</sup>	
<b>Refinement program</b>	SHELXL-2018/3 (Sheldrick, 2018)	
<b>Function minimized</b>	$\Sigma w(F_o^2 - F_c^2)^2$	
<b>Data / restraints / parameters</b>	6820 / 0 / 452	
<b>Goodness-of-fit on F<sup>2</sup></b>	1.204	
<b><math>\Delta/\sigma_{\max}</math></b>	0.000	
<b>Final R indices</b>	6820 data; I>2σ(I)	R1 = 0.0330, wR2 = 0.0653
	all data	R1 = 0.0429, wR2 = 0.0751
<b>Weighting scheme</b>	w=1/[σ <sup>2</sup> (F <sub>o</sub> <sup>2</sup> )+(0.0067P) <sup>2</sup> + 10.1039P] where P=(F <sub>o</sub> <sup>2</sup> +2F <sub>c</sub> <sup>2</sup> )/3	
<b>Largest diff. peak and hole</b>	1.024 and -0.573 eÅ <sup>-3</sup>	

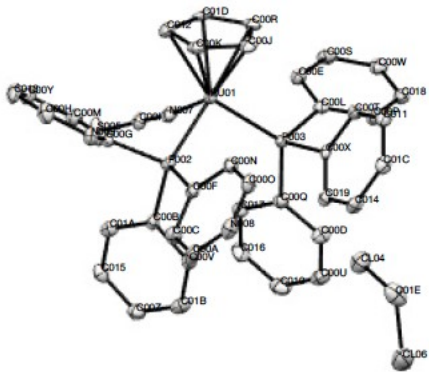


**Table S6. Bond lengths (Å) for 1a.**

Ru01 N007	2.064(5)	C00H C013	1.388(9)	C00Y C013	1.389(9)
Ru01 C01D	2.215(6)	C00H N009	1.396(8)	C00Y H00Y	0.9500
Ru01 C00K	2.216(6)	C00H H00H	0.9500	C00Z C015	1.381(10)
Ru01 C012	2.219(6)	C00J C00K	1.419(8)	C00Z C01B	1.391(8)
Ru01 C00J	2.230(6)	C00J C00R	1.456(8)	C00Z H00Z	0.9500
Ru01 C00R	2.230(6)	C00J H00J	0.9500	C01A C015	1.388(8)
Ru01 P003	2.3127(15)	C00K C012	1.424(9)	C01A H01A	0.9500
Ru01 P002	2.3169(15)	C00K H00K	0.9500	C01B H01B	0.9500
S005 C00I	1.629(6)	C00L C00P	1.410(8)	C01C C014	1.391(8)
P002 C00F	1.827(6)	C00M C00Y	1.384(8)	C01C C011	1.401(8)
P002 C00B	1.836(6)	C00M H00M	0.9500	C01C H01C	0.9500
P002 C00G	1.843(6)	C00N C00O	1.397(8)	C01D C012	1.438(9)
P003 C00X	1.830(6)	C00N H00N	0.9500	C01D H01D	0.9500
P003 C00L	1.836(6)	C00O N008	1.379(9)	C010 C016	1.387(9)
P003 C00Q	1.844(6)	C00O H00O	0.9500	C010 H010	0.9500
N007 C00I	1.162(7)	C00P C018	1.392(8)	C011 H011	0.9500
C00A N008	1.387(8)	C00P H00P	0.9500	C012 H012	0.9500
C00A C00C	1.394(9)	C00Q C017	1.404(8)	C013 H013	0.9500
C00A H00A	0.9500	C00R C01D	1.413(9)	C014 C019	1.386(8)
C00B C01A	1.386(8)	C00R H00R	0.9500	C014 H014	0.9500
C00B C00V	1.407(8)	C00S C00W	1.383(9)	C015 H015	0.9500
C00C C00F	1.404(8)	C00S H00S	0.9500	C016 C017	1.385(9)
C00C H00C	0.9500	C00T C011	1.383(8)	C016 H016	0.9500
C00D C00U	1.372(8)	C00T C00X	1.408(8)	C017 H017	0.9500
C00D C00Q	1.396(8)	C00T H00T	0.9500	C018 H018	0.9500

C00D H00D	0.9500	C00U C010	1.393(9)	C019 H019	0.9500
C00E C00L	1.398(8)	C00U H00U	0.9500	N008 H	0.9500
C00E C00S	1.399(8)	C00V C01B	1.386(8)	N009 HA	0.9500
C00E H00E	0.9500	C00V H00V	0.9500	Cl04 C01E	1.756(7)
C00F C00N	1.390(8)	C00W C018	1.389(9)	Cl06 C01E	1.763(7)
C00G N009	1.395(8)	C00W H00W	0.9500	C01E H01E	0.9900
C00G C00M	1.407(8)	C00X C019	1.398(8)	C01E H01F	0.9900

**Table S7. Bond angles (°) for 1a.**

N007 Ru01 C01D	90.8(2)	C00D C00Q C017	118.7(5)
N007 Ru01 C00K	133.1(2)	C00D C00Q P003	122.9(4)
C01D Ru01 C00K	62.5(2)	C017 C00Q P003	117.9(4)
N007 Ru01 C012	97.9(2)	C01D C00R C00J	108.4(5)
C01D Ru01 C012	37.8(2)	C01D C00R Ru01	70.9(3)
C00K Ru01 C012	37.5(2)	C00J C00R Ru01	70.9(3)
N007 Ru01 C00J	153.9(2)	C01D C00R H00R	125.8
C01D Ru01 C00J	63.1(2)	C00J C00R H00R	125.8
C00K Ru01 C00J	37.2(2)	Ru01 C00R H00R	124.0
C012 Ru01 C00J	63.1(2)	C00W C00S C00E	120.3(6)
N007 Ru01 C00R	118.5(2)	C00W C00S H00S	119.8
C01D Ru01 C00R	37.1(2)	C00E C00S H00S	119.8
C00K Ru01 C00R	62.3(2)	C011 C00T C00X	120.2(5)
C012 Ru01 C00R	62.7(2)	C011 C00T H00T	119.9
C00J Ru01 C00R	38.1(2)	C00X C00T H00T	119.9
N007 Ru01 P003	94.55(13)	C00D C00U C010	121.1(6)
C01D Ru01 P003	120.58(17)	C00D C00U H00U	119.4
C00K Ru01 P003	131.86(16)	C010 C00U H00U	119.4
C012 Ru01 P003	154.86(16)	C01B C00V C00B	121.3(6)
C00J Ru01 P003	97.40(16)	C01B C00V H00V	119.3
C00R Ru01 P003	92.19(16)	C00B C00V H00V	119.3
N007 Ru01 P002	87.22(14)	C00S C00W C018	119.9(5)
C01D Ru01 P002	140.63(17)	C00S C00W H00W	120.1
C00K Ru01 P002	91.10(16)	C018 C00W H00W	120.1
C012 Ru01 P002	103.59(17)	C019 C00X C00T	118.3(5)
C00J Ru01 P002	113.58(17)	C019 C00X P003	121.1(4)
C00R Ru01 P002	151.19(16)	C00T C00X P003	120.0(4)
P003 Ru01 P002	98.76(5)	C00M C00Y C013	120.1(6)
C00F P002 C00B	101.2(3)	C00M C00Y H00Y	120.0
C00F P002 C00G	102.6(3)	C013 C00Y H00Y	120.0
C00B P002 C00G	104.6(3)	C015 C00Z C01B	119.3(6)
C00F P002 Ru01	119.7(2)	C015 C00Z H00Z	120.3
C00B P002 Ru01	120.25(19)	C01B C00Z H00Z	120.3
C00G P002 Ru01	106.39(18)	C00B C01A C015	120.9(6)
C00X P003 C00L	102.7(3)	C00B C01A H01A	119.6

C00X P003 C00Q	104.9(3)	C015 C01A H01A	119.6
C00L P003 C00Q	95.2(3)	C00V C01B C00Z	119.8(6)
C00X P003 Ru01	111.73(18)	C00V C01B H01B	120.1
C00L P003 Ru01	114.68(19)	C00Z C01B H01B	120.1
C00Q P003 Ru01	124.50(19)	C014 C01C C011	119.2(5)
C00I N007 Ru01	168.8(4)	C014 C01C H01C	120.4
N008 C00A C00C	120.6(7)	C011 C01C H01C	120.4
N008 C00A H00A	119.7	C00R C01D C012	108.5(5)
C00C C00A H00A	119.7	C00R C01D Ru01	72.0(3)
C01A C00B C00V	117.8(5)	C012 C01D Ru01	71.2(3)
C01A C00B P002	123.9(5)	C00R C01D H01D	125.8
C00V C00B P002	118.2(4)	C012 C01D H01D	125.8
C00A C00C C00F	119.9(6)	Ru01 C01D H01D	122.7
C00A C00C H00C	120.0	C016 C010 C00U	118.4(6)
C00F C00C H00C	120.0	C016 C010 H010	120.8
C00U C00D C00Q	120.6(6)	C00U C010 H010	120.8
C00U C00D H00D	119.7	C00T C011 C01C	120.8(6)
C00Q C00D H00D	119.7	C00T C011 H011	119.6
C00L C00E C00S	120.6(5)	C01C C011 H011	119.6
C00L C00E H00E	119.7	C00K C012 C01D	106.9(5)
C00S C00E H00E	119.7	C00K C012 Ru01	71.2(3)
C00N C00F C00C	118.7(6)	C01D C012 Ru01	71.0(3)
C00N C00F P002	120.2(5)	C00K C012 H012	126.5
C00C C00F P002	121.2(5)	C01D C012 H012	126.5
N009 C00G C00M	117.5(5)	Ru01 C012 H012	123.0
N009 C00G P002	122.7(4)	C00H C013 C00Y	120.1(6)
C00M C00G P002	119.6(4)	C00H C013 H013	120.0
C013 C00H N009	119.3(6)	C00Y C013 H013	120.0
C013 C00H H00H	120.3	C019 C014 C01C	120.0(6)
N009 C00H H00H	120.3	C019 C014 H014	120.0
N007 C00I S005	179.1(6)	C01C C014 H014	120.0
C00K C00J C00R	106.2(5)	C00Z C015 C01A	120.9(6)
C00K C00J Ru01	70.9(3)	C00Z C015 H015	119.6
C00R C00J Ru01	71.0(3)	C01A C015 H015	119.6
C00K C00J H00J	126.9	C017 C016 C010	121.3(6)
C00R C00J H00J	126.9	C017 C016 H016	119.3

Ru01 C00J H00J	123.0	C010 C016 H016	119.3
C00J C00K C012	110.0(5)	C016 C017 C00Q	119.7(6)
C00J C00K Ru01	71.9(3)	C016 C017 H017	120.1
C012 C00K Ru01	71.4(3)	C00Q C017 H017	120.1
C00J C00K H00K	125.0	C00W C018 C00P	120.3(6)
C012 C00K H00K	125.0	C00W C018 H018	119.8
Ru01 C00K H00K	123.3	C00P C018 H018	119.8
C00E C00L C00P	118.4(5)	C014 C019 C00X	121.4(6)
C00E C00L P003	119.8(4)	C014 C019 H019	119.3
C00P C00L P003	121.1(5)	C00X C019 H019	119.3
C00Y C00M C00G	121.2(5)	C00O N008 C00A	119.8(6)
C00Y C00M H00M	119.4	C00O N008 H	120.1
C00G C00M H00M	119.4	C00A N008 H	120.1
C00F C00N C00O	121.0(6)	C00G N009 C00H	121.7(6)
C00F C00N H00N	119.5	C00G N009 HA	119.1
C00O C00N H00N	119.5	C00H N009 HA	119.1
N008 C00O C00N	119.9(6)	Cl04 C01E Cl06	111.8(4)
N008 C00O H00O	120.0	Cl04 C01E H01E	109.2
C00N C00O H00O	120.0	Cl06 C01E H01E	109.2
C018 C00P C00L	120.5(6)	Cl04 C01E H01F	109.2
C018 C00P H00P	119.8	Cl06 C01E H01F	109.2
C00L C00P H00P	119.8	H01E C01E H01F	107.9

**Table S8. Sample and crystal data for 2a.**

<b>Identification code</b>	TH110521_RK2_0m_a, CCDC 2282638	
<b>Chemical formula</b>	$C_{37}H_{33}NP_2RuS$	
<b>Formula weight</b>	772.04 g/mol	
<b>Temperature</b>	100(2) K	
<b>Wavelength</b>	0.71073 Å	
<b>Crystal size</b>	0.200 x 0.150 x 0.080 mm	
<b>Crystal habit</b>	clear light yellow prism	
<b>Crystal system</b>	triclinic	
<b>Space group</b>	P -1	
<b>Unit cell dimensions</b>	$a = 12.3722(4)$ Å	$\alpha = 91.665(2)^\circ$
	$b = 12.6828(4)$ Å	$\beta = 115.605(2)^\circ$
	$c = 13.5552(4)$ Å	$\gamma = 112.079(2)^\circ$
<b>Volume</b>	$1730.16(10)$ Å <sup>3</sup>	
<b>Z</b>	2	
<b>Density (calculated)</b>	1.483 g/cm <sup>3</sup>	
<b>Absorption coefficient</b>	0.789 mm <sup>-1</sup>	
<b>F(000)</b>	788	

**Table S9. Data collection and structure refinement for 2a.**

<b>Theta range for data collection</b>	2.738 to 26.616°	
<b>Index ranges</b>	-15<=h<=15, -15<=k<=15, -17<=l<=17	
<b>Reflections collected</b>	78119	
<b>Independent reflections</b>	7223 [R(int) = 0.0453]	
<b>Coverage of independent reflections</b>	99.5%	
<b>Absorption correction</b>	Multi-Scan	
<b>Max. and min. transmission</b>	0.833 and 0.928	
<b>Structure solution technique</b>	direct methods	
<b>Structure solution program</b>	SHELXL-2018/2 (Sheldrick, 2018)	
<b>Refinement method</b>	Full-matrix least-squares on F <sup>2</sup>	
<b>Refinement program</b>	SHELXL-2018/3 (Sheldrick, 2018)	
<b>Function minimized</b>	$\Sigma w(F_o^2 - F_c^2)^2$	
<b>Data / restraints / parameters</b>	7223 / 0 / 407	
<b>Goodness-of-fit on F<sup>2</sup></b>	1.089	
$\Delta/\sigma_{\max}$	0.001	
<b>Final R indices</b>	7223 data; I>2σ(I)	R1 = 0.0428, wR2 = 0.0798
	all data	R1 = 0.0712, wR2 = 0.0957
<b>Weighting scheme</b>	w=1/[σ <sup>2</sup> (F <sub>o</sub> <sup>2</sup> )+(0.0170P) <sup>2</sup> +5.9748P] where P=(F <sub>o</sub> <sup>2</sup> +2F <sub>c</sub> <sup>2</sup> )/3	
<b>Largest diff. peak and hole</b>	0.985 and -1.103 eÅ <sup>-3</sup>	

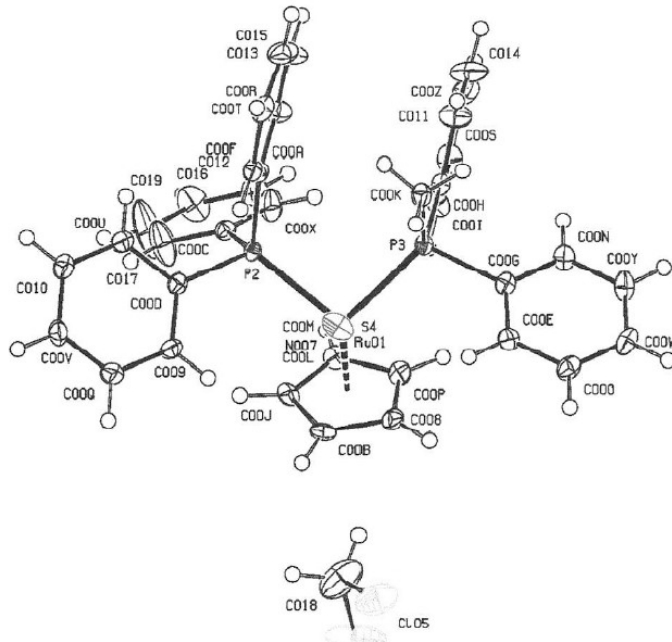


**Table S10. Bond lengths (Å) for 2a.**

Ru01 N007	2.065(3)	C008 C00P	1.422(5)	C00L C00P	1.417(5)
Ru01 C00L	2.197(4)	C008 C00B	1.429(5)	C00N C00Y	1.388(5)
Ru01 C00P	2.201(3)	C009 C00D	1.385(5)	C00O C00W	1.387(6)
Ru01 C00J	2.227(3)	C009 C00Q	1.391(5)	C00Q C00V	1.383(5)
Ru01 C008	2.233(4)	C00A C00R	1.393(5)	C00R C015	1.389(6)
Ru01 C00B	2.236(3)	C00A C00F	1.397(5)	C00S C00Z	1.385(6)
Ru01 P2	2.3078(9)	C00B C00J	1.420(5)	C00T C013	1.383(6)
Ru01 P3	2.3161(9)	C00C C00X	1.378(5)	C00U C010	1.383(5)
Cl05 C018	1.754(5)	C00C C017	1.382(6)	C00V C010	1.382(6)
Cl06 C018	1.749(5)	C00D C00U	1.402(5)	C00W C00Y	1.389(6)
S4 C00M	1.639(4)	C00E C00O	1.396(5)	C00Z C014	1.373(6)
P2 C00A	1.827(4)	C00E C00G	1.397(5)	C011 C014	1.391(6)
P2 C00D	1.832(4)	C00F C00T	1.389(5)	C012 C016	1.359(6)
P2 C00C	1.836(4)	C00G C00N	1.398(5)	C013 C015	1.382(6)
P3 C00K	1.825(4)	C00H C011	1.389(5)	C016 C019	1.378(7)
P3 C00H	1.834(4)	C00H C00I	1.397(5)	C017 C019	1.391(6)
P3 C00G	1.843(4)				
N007 C00M	1.156(5)				

**Table S11. Bond angles (°) for 2a.**

N007 Ru01 C00L	157.69(13)	C00J C00B Ru01	71.1(2)
N007 Ru01 C00P	137.44(13)	C008 C00B Ru01	71.2(2)
C00L Ru01 C00P	37.60(14)	C00X C00C C017	117.9(4)
N007 Ru01 C00J	121.31(13)	C00X C00C P2	118.5(3)
C00L Ru01 C00J	37.82(14)	C017 C00C P2	123.5(3)
C00P Ru01 C00J	62.39(14)	C009 C00D C00U	118.3(3)
N007 Ru01 C008	102.78(13)	C009 C00D P2	121.5(3)
C00L Ru01 C008	62.99(14)	C00U C00D P2	120.1(3)
C00P Ru01 C008	37.40(14)	C00O C00E C00G	121.1(4)
C00J Ru01 C008	62.31(14)	C00T C00F C00A	120.6(4)
N007 Ru01 C00B	95.22(13)	C00E C00G C00N	118.3(3)
C00L Ru01 C00B	62.88(14)	C00E C00G P3	117.7(3)
C00P Ru01 C00B	62.32(14)	C00N C00G P3	123.7(3)
C00J Ru01 C00B	37.11(13)	C011 C00H C00I	117.8(4)
C008 Ru01 C00B	37.30(14)	C011 C00H P3	122.4(3)
N007 Ru01 P2	87.91(8)	C00I C00H P3	119.7(3)
C00L Ru01 P2	98.66(10)	C00S C00I C00H	121.4(4)
C00P Ru01 P2	134.17(11)	C00B C00J C00L	108.2(3)
C00J Ru01 P2	91.39(10)	C00B C00J Ru01	71.8(2)
C008 Ru01 P2	153.53(10)	C00L C00J Ru01	69.9(2)
C00B Ru01 P2	118.57(10)	C00P C00L C00J	107.1(3)
N007 Ru01 P3	86.56(9)	C00P C00L Ru01	71.3(2)
C00L Ru01 P3	113.42(10)	C00J C00L Ru01	72.3(2)
C00P Ru01 P3	92.57(10)	N007 C00M S4	178.2(4)
C00J Ru01 P3	151.14(10)	C00Y C00N C00G	120.4(4)
C008 Ru01 P3	107.19(10)	C00W C00O C00E	119.9(4)
C00B Ru01 P3	143.95(10)	C00L C00P C008	109.2(3)
P2 Ru01 P3	97.46(3)	C00L C00P Ru01	71.1(2)
C00A P2 C00D	100.62(16)	C008 C00P Ru01	72.5(2)
C00A P2 C00C	104.58(16)	C00V C00Q C009	120.2(4)
C00D P2 C00C	102.20(16)	C015 C00R C00A	120.7(4)
C00A P2 Ru01	119.41(11)	C00I C00S C00Z	119.9(4)
C00D P2 Ru01	115.18(12)	C013 C00T C00F	120.1(4)
C00C P2 Ru01	112.73(12)	C010 C00U C00D	120.8(4)

C00K P3 C00H	103.49(17)	C010 C00V C00Q	119.7(4)
C00K P3 C00G	98.37(16)	C00O C00W C00Y	119.4(4)
C00H P3 C00G	102.71(16)	C00C C00X C012	121.9(4)
C00K P3 Ru01	118.70(12)	C00N C00Y C00W	120.8(4)
C00H P3 Ru01	118.92(12)	C014 C00Z C00S	119.5(4)
C00G P3 Ru01	111.66(12)	C00V C010 C00U	120.2(4)
C00M N007 Ru01	173.8(3)	C00H C011 C014	120.6(4)
C00P C008 C00B	107.3(3)	C016 C012 C00X	120.3(4)
C00P C008 Ru01	70.1(2)	C015 C013 C00T	119.9(4)
C00B C008 Ru01	71.5(2)	C00Z C014 C011	120.7(4)
C00D C009 C00Q	120.8(3)	C013 C015 C00R	120.2(4)
C00R C00A C00F	118.5(3)	C012 C016 C019	118.6(4)
C00R C00A P2	122.6(3)	C00C C017 C019	119.8(4)
C00F C00A P2	118.7(3)	Cl06 C018 Cl05	113.4(3)
C00J C00B C008	108.1(3)	C016 C019 C017	121.6(5)

**Table S12. Sample and crystal data for 3b.**

<b>Identification code</b>	Kirss2, CCDC 2282639	
<b>Chemical formula</b>	$C_{42}H_{35}NP_2RuSe$	
<b>Formula weight</b>	795.68 g/mol	
<b>Temperature</b>	100.0(5) K	
<b>Wavelength</b>	0.71073 Å	
<b>Crystal size</b>	0.320 x 0.170 x 0.020 mm	
<b>Crystal habit</b>	Orange lath	
<b>Crystal system</b>	monoclinic	
<b>Space group</b>	P 2 <sub>1</sub> /c	
<b>Unit cell dimensions</b>	a = 18.2161(14) Å	α = 90°
	b = 10.9631(8) Å	β = 114.698(2)
	c = 18.8210(15) Å	γ = 90°
<b>Volume</b>	3414.8(5) Å <sup>3</sup>	
<b>Z</b>	4	
<b>Density (calculated)</b>	1.548 g/cm <sup>3</sup>	
<b>Absorption coefficient</b>	1.651 mm <sup>-1</sup>	
<b>F(000)</b>	1608	

**Table S13. Data collection and structure refinement for 3b.**

<b>Theta range for data collection</b>	1.23 to 30.61°	
<b>Index ranges</b>	-26<=h<=26, -15<=k<=15, -26<=l<=26	
<b>Reflections collected</b>	52316	
<b>Independent reflections</b>	10479 [R(int) = 0.1087]	
<b>Coverage of independent reflections</b>	99.5%	
<b>Absorption correction</b>	Multi-Scan	
<b>Max. and min. transmission</b>	0.866 and 0.968	
<b>Structure solution technique</b>	direct methods	
<b>Structure solution program</b>	SHELXT 2014/5 (Sheldrick, 2014)	
<b>Refinement method</b>	Full-matrix least-squares on F <sup>2</sup>	
<b>Refinement program</b>	SHELXL-2017/1 (Sheldrick, 2017)	
<b>Function minimized</b>	$\Sigma w(F_o^2 - F_c^2)^2$	
<b>Data / restraints / parameters</b>	10479 / 0 / 424	
<b>Goodness-of-fit on F<sup>2</sup></b>	0.999	
<b><math>\Delta/\sigma_{\max}</math></b>	0.001	
<b>Final R indices</b>	10479 data; I>2σ(I)	R1 = 0.0514, wR2 = 0.0783
	all data	R1 = 0.1094, wR2 = 0.09300
<b>Weighting scheme</b>	w=1/[σ <sup>2</sup> (F <sub>o</sub> <sup>2</sup> )+(0.0276P) <sup>2</sup> +1.2500P] where P=(F <sub>o</sub> <sup>2</sup> +2F <sub>c</sub> <sup>2</sup> )/3	
<b>Largest diff. peak and hole</b>	0.768 and -0.719 eÅ <sup>-3</sup>	

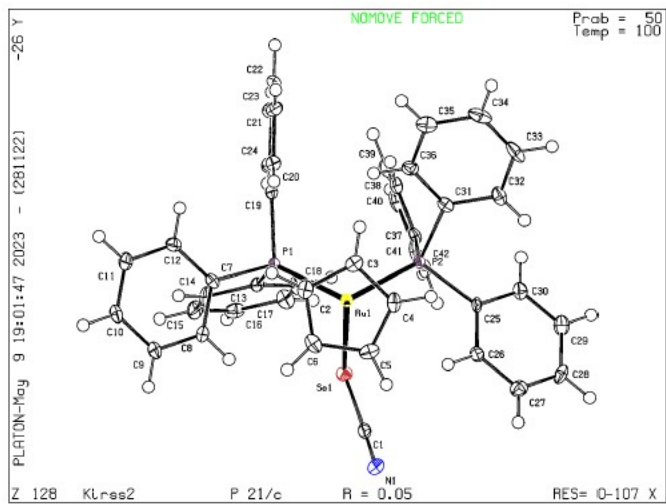


**Table S14. Bond lengths (Å) for 3b.**

Ru1 C3	2.202(3)	C9 H9	0.9500	C26 H26	0.9500
Ru1 C5	2.205(3)	C10 C11	1.378(5)	C27 C28	1.373(5)
Ru1 C2	2.207(3)	C10 H10	0.9500	C27 H27	0.9500
Ru1 C4	2.210(3)	C11 C12	1.392(5)	C28 C29	1.381(5)
Ru1 C6	2.211(3)	C11 H11	0.9500	C28 H28	0.9500
Ru1 P2	2.3423(9)	C12 H12	0.9500	C29 C30	1.378(5)
Ru1 P1	2.3493(9)	C13 C18	1.390(5)	C29 H29	0.9500
Ru1 Se1	2.5424(5)	C13 C14	1.395(5)	C30 H30	0.9500
Se1 C1	1.850(4)	C14 C15	1.382(5)	C31 C36	1.388(5)
P1 C19	1.836(4)	C14 H14	0.9500	C31 C32	1.402(5)
P1 C7	1.838(3)	C15 C16	1.393(5)	C32 C33	1.382(5)
P1 C13	1.843(3)	C15 H15	0.9500	C32 H32	0.9500
P2 C37	1.836(3)	C16 C17	1.377(5)	C33 C34	1.379(6)
P2 C25	1.843(4)	C16 H16	0.9500	C33 H33	0.9500
P2 C31	1.845(4)	C17 C18	1.387(5)	C34 C35	1.384(5)
N1 C1	1.147(5)	C17 H17	0.9500	C34 H34	0.9500
C2 C6	1.400(5)	C18 H18	0.9500	C35 C36	1.383(5)
C2 C3	1.410(5)	C19 C24	1.391(5)	C35 H35	0.9500
C2 H2	0.9500	C19 C20	1.397(5)	C36 H36	0.9500
C3 C4	1.423(5)	C20 C21	1.381(5)	C37 C38	1.380(5)
C3 H3	0.9500	C20 H20	0.9500	C37 C42	1.402(5)
C4 C5	1.407(5)	C21 C22	1.390(5)	C38 C39	1.388(5)
C4 H4	0.9500	C21 H21	0.9500	C38 H38	0.9500

C5 C6	1.433(5)	C22 C23	1.378(6)	C39 C40	1.380(5)
C5 H5	0.9500	C22 H22	0.9500	C39 H39	0.9500
C6 H6	0.9500	C23 C24	1.387(5)	C40 C41	1.384(5)
C7 C12	1.392(5)	C23 H23	0.9500	C40 H40	0.9500
C7 C8	1.393(5)	C24 H24	0.9500	C41 C42	1.387(5)
C8 C9	1.383(5)	C25 C26	1.388(5)	C41 H41	0.9500
C8 H8	0.9500	C25 C30	1.405(4)	C42 H42	0.9500
C9 C10	1.377(5)	C26 C27	1.391(5)		

**Table S15. Bond angles (°) for 3b.**

C3 Ru1 C5	62.50(13)	C18 C13 C14	118.3(3)
C3 Ru1 C2	37.30(13)	C18 C13 P1	118.8(3)
C5 Ru1 C2	62.21(13)	C14 C13 P1	122.9(3)
C3 Ru1 C4	37.63(13)	C15 C14 C13	120.5(3)
C5 Ru1 C4	37.16(13)	C15 C14 H14	119.7
C2 Ru1 C4	62.34(13)	C13 C14 H14	119.7
C3 Ru1 C6	62.53(14)	C14 C15 C16	120.3(3)
C5 Ru1 C6	37.88(13)	C14 C15 H15	119.8
C2 Ru1 C6	36.94(13)	C16 C15 H15	119.8
C4 Ru1 C6	62.74(13)	C17 C16 C15	119.8(3)
C3 Ru1 P2	99.46(10)	C17 C16 H16	120.1
C5 Ru1 P2	113.02(10)	C15 C16 H16	120.1
C2 Ru1 P2	135.92(10)	C16 C17 C18	119.7(3)
C4 Ru1 P2	87.89(9)	C16 C17 H17	120.1
C6 Ru1 P2	149.62(10)	C18 C17 H17	120.1
C3 Ru1 P1	109.65(10)	C17 C18 C13	121.4(3)
C5 Ru1 P1	143.34(10)	C17 C18 H18	119.3
C2 Ru1 P1	89.65(10)	C13 C18 H18	119.3
C4 Ru1 P1	147.24(10)	C24 C19 C20	118.5(3)
C6 Ru1 P1	105.60(10)	C24 C19 P1	123.2(3)
P2 Ru1 P1	103.52(3)	C20 C19 P1	118.3(3)
C3 Ru1 Se1	157.65(10)	C21 C20 C19	121.0(4)
C5 Ru1 Se1	95.26(10)	C21 C20 H20	119.5
C2 Ru1 Se1	132.01(10)	C19 C20 H20	119.5
C4 Ru1 Se1	124.32(10)	C20 C21 C22	119.8(4)
C6 Ru1 Se1	98.99(10)	C20 C21 H21	120.1
P2 Ru1 Se1	91.15(3)	C22 C21 H21	120.1
P1 Ru1 Se1	86.58(3)	C23 C22 C21	119.8(4)
C1 Se1 Ru1	100.90(11)	C23 C22 H22	120.1
C19 P1 C7	102.98(16)	C21 C22 H22	120.1
C19 P1 C13	102.64(16)	C22 C23 C24	120.5(4)
C7 P1 C13	98.99(15)	C22 C23 H23	119.7
C19 P1 Ru1	116.53(12)	C24 C23 H23	119.7
C7 P1 Ru1	111.20(11)	C23 C24 C19	120.4(4)
C13 P1 Ru1	121.69(11)	C23 C24 H24	119.8

C37 P2 C25	99.91(16)	C19 C24 H24	119.8
C37 P2 C31	101.67(15)	C26 C25 C30	118.1(3)
C25 P2 C31	103.14(16)	C26 C25 P2	120.0(2)
C37 P2 Ru1	121.96(11)	C30 C25 P2	121.9(3)
C25 P2 Ru1	114.66(12)	C25 C26 C27	120.8(3)
C31 P2 Ru1	112.97(11)	C25 C26 H26	119.6
N1 C1 Se1	178.3(3)	C27 C26 H26	119.6
C6 C2 C3	109.2(3)	C28 C27 C26	120.4(4)
C6 C2 Ru1	71.7(2)	C28 C27 H27	119.8
C3 C2 Ru1	71.17(19)	C26 C27 H27	119.8
C6 C2 H2	125.4	C27 C28 C29	119.6(3)
C3 C2 H2	125.4	C27 C28 H28	120.2
Ru1 C2 H2	123.4	C29 C28 H28	120.2
C2 C3 C4	107.6(3)	C30 C29 C28	120.7(3)
C2 C3 Ru1	71.5(2)	C30 C29 H29	119.7
C4 C3 Ru1	71.48(19)	C28 C29 H29	119.7
C2 C3 H3	126.2	C29 C30 C25	120.5(4)
C4 C3 H3	126.2	C29 C30 H30	119.7
Ru1 C3 H3	122.5	C25 C30 H30	119.7
C5 C4 C3	107.8(3)	C36 C31 C32	117.8(3)
C5 C4 Ru1	71.2(2)	C36 C31 P2	117.8(3)
C3 C4 Ru1	70.90(19)	C32 C31 P2	124.5(3)
C5 C4 H4	126.1	C33 C32 C31	120.4(4)
C3 C4 H4	126.1	C33 C32 H32	119.8
Ru1 C4 H4	123.4	C31 C32 H32	119.8
C4 C5 C6	108.2(3)	C34 C33 C32	121.0(4)
C4 C5 Ru1	71.6(2)	C34 C33 H33	119.5
C6 C5 Ru1	71.3(2)	C32 C33 H33	119.5
C4 C5 H5	125.9	C33 C34 C35	119.2(4)
C6 C5 H5	125.9	C33 C34 H34	120.4
Ru1 C5 H5	122.9	C35 C34 H34	120.4
C2 C6 C5	107.1(3)	C36 C35 C34	120.0(4)
C2 C6 Ru1	71.4(2)	C36 C35 H35	120.0
C5 C6 Ru1	70.84(19)	C34 C35 H35	120.0
C2 C6 H6	126.4	C35 C36 C31	121.6(3)
C5 C6 H6	126.4	C35 C36 H36	119.2

Ru1 C6 H6	123.0	C31 C36 H36	119.2
C12 C7 C8	118.5(3)	C38 C37 C42	118.3(3)
C12 C7 P1	123.9(3)	C38 C37 P2	121.4(3)
C8 C7 P1	117.5(3)	C42 C37 P2	119.9(3)
C9 C8 C7	121.1(3)	C37 C38 C39	120.8(3)
C9 C8 H8	119.5	C37 C38 H38	119.6
C7 C8 H8	119.5	C39 C38 H38	119.6
C10 C9 C8	120.0(4)	C40 C39 C38	120.6(4)
C10 C9 H9	120.0	C40 C39 H39	119.7
C8 C9 H9	120.0	C38 C39 H39	119.7
C9 C10 C11	119.8(3)	C39 C40 C41	119.4(3)
C9 C10 H10	120.1	C39 C40 H40	120.3
C11 C10 H10	120.1	C41 C40 H40	120.3
C10 C11 C12	120.6(4)	C40 C41 C42	120.1(4)
C10 C11 H11	119.7	C40 C41 H41	119.9
C12 C11 H11	119.7	C42 C41 H41	119.9
C7 C12 C11	120.1(3)	C41 C42 C37	120.8(4)
C7 C12 H12	120.0	C41 C42 H42	119.6
C11 C12 H12	120.0	C37 C42 H42	119.6

**Table S16. Sample and crystal data for 4b.**

<b>Identification code</b>	Kirss2, CCDC 2282640	
<b>Chemical formula</b>	$C_{37}H_{33}NP_2RuSe$	
<b>Formula weight</b>	731.61 g/mol	
<b>Temperature</b>	150 K	
<b>Wavelength</b>	0.71073 Å	
<b>Crystal size</b>	0.22 x 0.21 x 0.06 mm	
<b>Crystal habit</b>	Orange plate	
<b>Crystal system</b>	orthorhombic	
<b>Space group</b>	Pna2 <sub>1</sub>	
<b>Unit cell dimensions</b>	a = 13.1668(9) Å	α = 90°
	b = 21.2752(12) Å	β = 114.698(2)
	c = 11.1139(3) Å	γ = 90°
<b>Volume</b>	3113.3(3) Å <sup>3</sup>	
<b>Z</b>	4	
<b>Density (calculated)</b>	1.565 g/cm <sup>3</sup>	
<b>Absorption coefficient</b>	1.80 mm <sup>-1</sup>	
<b>F(000)</b>	1480	

**Table S17. Data collection and structure refinement for 4b.**

<b>Theta range for data collection</b>	1.8 to 28.4°	
<b>Index ranges</b>	-17<=h<=11, -27<=k<=28, -14<=l<=14	
<b>Reflections collected</b>	33888	
<b>Independent reflections</b>	7747 [R(int) = 0.101]	
<b>Coverage of independent reflections</b>	99.5%	
<b>Absorption correction</b>	Multi-Scan	
<b>Max. and min. transmission</b>	0.769 and 0.900	
<b>Structure solution technique</b>	direct methods	
<b>Structure solution program</b>	SHELXT 2014/5 (Sheldrick, 2014)	
<b>Refinement method</b>	Full-matrix least-squares on $F^2$	
<b>Refinement program</b>	SHELXL-2017/1 (Sheldrick, 2017)	
<b>Function minimized</b>	$\Sigma w(F_o^2 - F_c^2)^2$	
<b>Data / restraints / parameters</b>	7747 / 147 / 237	
<b>Goodness-of-fit on <math>F^2</math></b>	1.17	
$\Delta/\sigma_{\max}$	0.001	
<b>Final R indices</b>	5305 data; I>2σ(I)	R1 = 0.106, wR2 = 0.227
<b>Weighting scheme</b>	w=1/[σ²(F₀²)+39.579P] where P=(F₀²+2Fc²)/3	
<b>Largest diff. peak and hole</b>	0.90 and -1.99 eÅ⁻³	

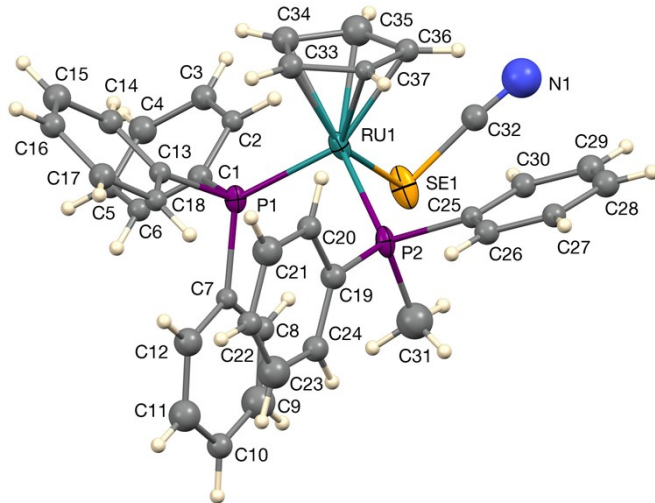


**Table S18. Bond lengths (Å) for 4b.**

Ru1 C33	2.197(15)	C22 H22	0.9500	C7A C12A	1.3900
Ru1 C35	2.216(16)	C23 C24	1.3900	C8A C9A	1.3900
Ru1 C34	2.217(15)	C23 H23	0.9500	C8A H8A	0.9500
Ru1 C37	2.230(15)	C24 H24	0.9500	C9A C10A	1.3900
Ru1 C36	2.235(15)	C25 C26	1.3900	C9A H9A	0.9500
Ru1 P1	2.276(8)	C25 C30	1.3900	C10A C11A	1.3900
Ru1 P2	2.292(7)	C26 C27	1.3900	C10A H10A	0.9500
Ru1 Se1	2.542(4)	C26 H26	0.9500	C11A C12A	1.3900
Se1 C32	1.8506(13)	C27 C28	1.3900	C11A H11A	0.9500
P1 C13	1.841(10)	C27 H27	0.9500	C12A H12A	0.9500
P1 C7	1.867(10)	C28 C29	1.3900	C13A C14A	1.3900
P1 C1	1.869(10)	C28 H28	0.9500	C13A C18A	1.3900
P2 C31	1.83(2)	C29 C30	1.3900	C14A C15A	1.3900
P2 C19	1.834(10)	C29 H29	0.9500	C14A H14A	0.9500
P2 C25	1.869(10)	C30 H30	0.9500	C15A C16A	1.3900
N1 C32	1.1476(13)	C31 H31A	0.9800	C15A H15A	0.9500
C1 C2	1.3900	C31 H31B	0.9800	C16A C17A	1.3900
C1 C6	1.3900	C31 H31C	0.9800	C16A H16A	0.9500
C2 C3	1.3900	C33 C34	1.421(18)	C17A C18A	1.3900
C2 H2	0.9500	C33 C37	1.422(17)	C17A H17A	0.9500
C3 C4	1.3900	C33 H33	0.9500	C18A H18A	0.9500
C3 H3	0.9500	C34 C35	1.417(19)	C19A C20A	1.3900
C4 C5	1.3900	C34 H34	0.9500	C19A C24A	1.3900
C4 H4	0.9500	C35 C36	1.405(18)	C20A C21A	1.3900
C5 C6	1.3900	C35 H35	0.9500	C20A H20A	0.9500
C5 H5	0.9500	C36 C37	1.433(17)	C21A C22A	1.3900
C6 H6	0.9500	C36 H36	0.9500	C21A H21A	0.9500
C7 C8	1.3900	C37 H37	0.9500	C22A C23A	1.3900
C7 C12	1.3900	Ru1A C36A	2.210(19)	C22A H22A	0.9500
C8 C9	1.3900	Ru1A C33A	2.21(2)	C23A C24A	1.3900
C8 H8	0.9500	Ru1A C34A	2.22(2)	C23A H23A	0.9500
C9 C10	1.3900	Ru1A C37A	2.22(2)	C24A H24A	0.9500
C9 H9	0.9500	Ru1A C35A	2.23(2)	C25A C26A	1.3900
C10 C11	1.3900	Ru1A P2A	2.284(13)	C25A C30A	1.3900
C10 H10	0.9500	Ru1A P1A	2.308(19)	C26A C27A	1.3900

C11 C12	1.3900	Ru1A Se1A	2.536(7)	C26A H26A	0.9500
C11 H11	0.9500	Se1A C32A	1.8502(14)	C27A C28A	1.3900
C12 H12	0.9500	P1A C13A	1.843(17)	C27A H27A	0.9500
C13 C14	1.3900	P1A C1A	1.861(17)	C28A C29A	1.3900
C13 C18	1.3900	P1A C7A	1.872(17)	C28A H28A	0.9500
C14 C15	1.3900	P2A C31A	1.83(3)	C29A C30A	1.3900
C14 H14	0.9500	P2A C19A	1.850(16)	C29A H29A	0.9500
C15 C16	1.3900	P2A C25A	1.855(16)	C30A H30A	0.9500
C15 H15	0.9500	N1A C32A	1.1472(13)	C31A H31D	0.9800
C16 C17	1.3900	C1A C2A	1.3900	C31A H31E	0.9800
C16 H16	0.9500	C1A C6A	1.3900	C31A H31F	0.9800
C17 C18	1.3900	C2A C3A	1.3900	C33A C37A	1.42(2)
C17 H17	0.9500	C2A H2A	0.9500	C33A C34A	1.43(2)
C18 H18	0.9500	C3A C4A	1.3900	C33A H33A	0.9500
C19 C20	1.3900	C3A H3A	0.9500	C34A C35A	1.43(2)
C19 C24	1.3900	C4A C5A	1.3900	C34A H34A	0.9500
C20 C21	1.3900	C4A H4A	0.9500	C35A C36A	1.42(2)
C20 H20	0.9500	C5A C6A	1.3900	C35A H35A	0.9500
C21 C22	1.3900	C5A H5A	0.9500	C36A C37A	1.43(2)
C21 H21	0.9500	C6A H6A	0.9500	C36A H36A	0.9500
C22 C23	1.3900	C7A C8A	1.3900	C37A H37A	0.9500

**Table S19. Bond angles (°) for 4b.**

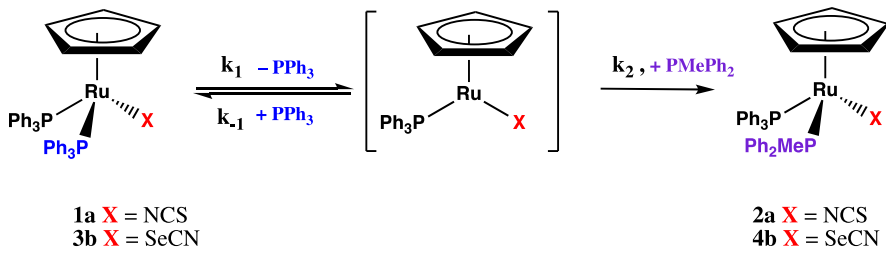
C33 Ru1 C35	62.0(8)	C36A Ru1A C33A	64.2(13)
C33 Ru1 C34	37.6(5)	C36A Ru1A C34A	63.5(13)
C35 Ru1 C34	37.3(5)	C33A Ru1A C34A	37.6(6)
C33 Ru1 C37	37.5(5)	C36A Ru1A C37A	37.5(6)
C35 Ru1 C37	61.0(8)	C33A Ru1A C37A	37.5(6)
C34 Ru1 C37	62.2(7)	C34A Ru1A C37A	61.6(14)
C33 Ru1 C36	63.4(7)	C36A Ru1A C35A	37.5(6)
C35 Ru1 C36	36.8(5)	C33A Ru1A C35A	62.8(12)
C34 Ru1 C36	63.1(7)	C34A Ru1A C35A	37.5(6)
C37 Ru1 C36	37.4(5)	C37A Ru1A C35A	61.2(15)
C33 Ru1 P1	96.6(6)	C36A Ru1A P2A	141.3(10)
C35 Ru1 P1	119.0(6)	C33A Ru1A P2A	110.0(11)
C34 Ru1 P1	90.0(6)	C34A Ru1A P2A	88.6(13)
C37 Ru1 P1	131.9(5)	C37A Ru1A P2A	147.1(11)
C36 Ru1 P1	153.0(6)	C35A Ru1A P2A	104.3(11)
C33 Ru1 P2	111.9(5)	C36A Ru1A P1A	121.4(10)
C35 Ru1 P2	143.8(6)	C33A Ru1A P1A	99.0(12)
C34 Ru1 P2	149.4(5)	C34A Ru1A P1A	133.7(12)
C37 Ru1 P2	92.0(5)	C37A Ru1A P1A	94.4(12)
C36 Ru1 P2	107.2(5)	C35A Ru1A P1A	155.5(12)
P1 Ru1 P2	96.9(3)	P2A Ru1A P1A	97.1(5)
C33 Ru1 Se1	154.8(5)	C36A Ru1A Se1A	91.0(10)
C35 Ru1 Se1	93.2(6)	C33A Ru1A Se1A	154.9(10)
C34 Ru1 Se1	119.2(5)	C34A Ru1A Se1A	135.3(11)
C37 Ru1 Se1	135.4(4)	C37A Ru1A Se1A	119.2(9)
C36 Ru1 Se1	100.0(5)	C35A Ru1A Se1A	100.2(11)
P1 Ru1 Se1	91.8(2)	P2A Ru1A Se1A	91.5(4)
P2 Ru1 Se1	90.5(2)	P1A Ru1A Se1A	90.7(4)
C32 Se1 Ru1	99.6(6)	C32A Se1A Ru1A	102.4(12)
C13 P1 C7	104.6(8)	C13A P1A C1A	100.8(19)
C13 P1 C1	101.8(8)	C13A P1A C7A	107.1(18)
C7 P1 C1	95.9(8)	C1A P1A C7A	99.0(17)
C13 P1 Ru1	111.5(6)	C13A P1A Ru1A	122.6(14)
C7 P1 Ru1	122.3(6)	C1A P1A Ru1A	114.4(13)
C1 P1 Ru1	117.8(6)	C7A P1A Ru1A	110.1(13)
C31 P2 C19	105.7(12)	C31A P2A C19A	100(2)
C31 P2 C25	99.8(12)	C31A P2A C25A	98(2)
C19 P2 C25	101.3(8)	C19A P2A C25A	104.0(17)
C31 P2 Ru1	118.6(10)	C31A P2A Ru1A	121(2)
C19 P2 Ru1	118.1(7)	C19A P2A Ru1A	118.3(14)
C25 P2 Ru1	110.6(6)	C25A P2A Ru1A	112.8(12)
C2 C1 C6	120.0	C2A C1A C6A	120.0
C2 C1 P1	117.4(9)	C4A C3A C2A	120.0
C6 C1 P1	122.2(9)	C4A C3A H3A	120.0
C3 C2 C1	120.0	C2A C3A H3A	120.0
C3 C2 H2	120.0	C3A C4A C5A	120.0
C1 C2 H2	120.0	C3A C4A H4A	120.0
C2 C3 C4	120.0	C5A C4A H4A	120.0
C2 C3 H3	120.0	C4A C5A C6A	120.0
C4 C3 H3	120.0	C4A C5A H5A	120.0
C5 C4 C3	120.0	C6A C5A H5A	120.0

C5 C4 H4	120.0	C5A C6A C1A	120.0
C3 C4 H4	120.0	C5A C6A H6A	120.0
C4 C5 C6	120.0	C1A C6A H6A	120.0
C4 C5 H5	120.0	C8A C7A C12A	120.0
C6 C5 H5	120.0	C8A C7A P1A	118.7(18)
C5 C6 C1	120.0	C12A C7A P1A	121.3(18)
C5 C6 H6	120.0	C9A C8A C7A	120.0
C1 C6 H6	120.0	C9A C8A H8A	120.0
C8 C7 C12	120.0	C7A C8A H8A	120.0
C8 C7 P1	115.6(9)	C8A C9A C10A	120.0
C12 C7 P1	124.4(9)	C8A C9A H9A	120.0
C9 C8 C7	120.0	C10A C9A H9A	120.0
C9 C8 H8	120.0	C11A C10A C9A	120.0
C7 C8 H8	120.0	C11A C10A H10A	120.0
C10 C9 C8	120.0	C9A C10A H10A	120.0
C10 C9 H9	120.0	C10A C11A C12A	120.0
C8 C9 H9	120.0	C10A C11A H11A	120.0
C9 C10 C11	120.0	C12A C11A H11A	120.0
C9 C10 H10	120.0	C11A C12A C7A	120.0
C11 C10 H10	120.0	C11A C12A H12A	120.0
C10 C11 C12	120.0	C7A C12A H12A	120.0
C10 C11 H11	120.0	C14A C13A C18A	120.0
C12 C11 H11	120.0	C14A C13A P1A	116(2)
C11 C12 C7	120.0	C18A C13A P1A	124(2)
C11 C12 H12	120.0	C15A C14A C13A	120.0
C7 C12 H12	120.0	C15A C14A H14A	120.0
C14 C13 C18	120.0	C13A C14A H14A	120.0
C14 C13 P1	120.4(8)	C16A C15A C14A	120.0
C18 C13 P1	119.4(8)	C16A C15A H15A	120.0
C13 C14 C15	120.0	C14A C15A H15A	120.0
C13 C14 H14	120.0	C15A C16A C17A	120.0
C15 C14 H14	120.0	C15A C16A H16A	120.0
C16 C15 C14	120.0	C17A C16A H16A	120.0
C16 C15 H15	120.0	C18A C17A C16A	120.0
C14 C15 H15	120.0	C18A C17A H17A	120.0
C17 C16 C15	120.0	C16A C17A H17A	120.0
C17 C16 H16	120.0	C17A C18A C13A	120.0
C15 C16 H16	120.0	C17A C18A H18A	120.0
C16 C17 C18	120.0	C13A C18A H18A	120.0
C16 C17 H17	120.0	C20A C19A C24A	120.0
C18 C17 H17	120.0	C20A C19A P2A	123(2)
C17 C18 C13	120.0	C24A C19A P2A	117(2)
C17 C18 H18	120.0	C21A C20A C19A	120.0
C13 C18 H18	120.0	C21A C20A H20A	120.0
C20 C19 C24	120.0	C19A C20A H20A	120.0
C20 C19 P2	118.0(10)	C20A C21A C22A	120.0
C24 C19 P2	122.0(10)	C20A C21A H21A	120.0
C19 C20 C21	120.0	C22A C21A H21A	120.0
C19 C20 H20	120.0	C21A C22A C23A	120.0
C21 C20 H20	120.0	C21A C22A H22A	120.0
C20 C21 C22	120.0	C23A C22A H22A	120.0
C20 C21 H21	120.0	C24A C23A C22A	120.0
C22 C21 H21	120.0	C24A C23A H23A	120.0

C23 C22 C21	120.0	C22A C23A H23A	120.0
C23 C22 H22	120.0	C23A C24A C19A	120.0
C21 C22 H22	120.0	C23A C24A H24A	120.0
C24 C23 C22	120.0	C19A C24A H24A	120.0
C24 C23 H23	120.0	C26A C25A C30A	120.0
C22 C23 H23	120.0	C26A C25A P2A	117.5(17)
C23 C24 C19	120.0	C30A C25A P2A	122.4(17)
C23 C24 H24	120.0	C25A C26A C27A	120.0
C19 C24 H24	120.0	C25A C26A H26A	120.0
C26 C25 C30	120.0	C27A C26A H26A	120.0
C26 C25 P2	123.7(8)	C26A C27A C28A	120.0
C30 C25 P2	116.2(8)	C26A C27A H27A	120.0
C27 C26 C25	120.0	C28A C27A H27A	120.0
C27 C26 H26	120.0	C29A C28A C27A	120.0
C25 C26 H26	120.0	C29A C28A H28A	120.0
C26 C27 C28	120.0	C27A C28A H28A	120.0
C26 C27 H27	120.0	C30A C29A C28A	120.0
C28 C27 H27	120.0	C30A C29A H29A	120.0
C29 C28 C27	120.0	C28A C29A H29A	120.0
C29 C28 H28	120.0	C29A C30A C25A	120.0
C27 C28 H28	120.0	C29A C30A H30A	120.0
C30 C29 C28	120.0	C25A C30A H30A	120.0
C30 C29 H29	120.0	P2A C31A H31D	109.5
C28 C29 H29	120.0	P2A C31A H31E	109.5
C29 C30 C25	120.0	H31D C31A H31E	109.5
C29 C30 H30	120.0	P2A C31A H31F	109.5
C25 C30 H30	120.0	H31D C31A H31F	109.5
P2 C31 H31A	109.5	H31E C31A H31F	109.5
P2 C31 H31B	109.5	N1A C32A Se1A	177(3)
H31A C31 H31B	109.5	C37A C33A C34A	106(3)
P2 C31 H31C	109.5	C37A C33A Ru1A	71.5(10)
H31A C31 H31C	109.5	C34A C33A Ru1A	71.3(10)
H31B C31 H31C	109.5	C37A C33A H33A	127.1
N1 C32 Se1	175.5(17)	C34A C33A H33A	127.1
C34 C33 C37	107.8(16)	Ru1A C33A H33A	121.8
C34 C33 Ru1	72.0(8)	C35A C34A C33A	108(3)
C37 C33 Ru1	72.5(8)	C35A C34A Ru1A	71.6(10)
C34 C33 H33	126.1	C33A C34A Ru1A	71.1(10)
C37 C33 H33	126.1	C35A C34A H34A	125.8
Ru1 C33 H33	121.1	C33A C34A H34A	125.8
C35 C34 C33	106.4(17)	Ru1A C34A H34A	123.1
C35 C34 Ru1	71.3(8)	C36A C35A C34A	109(3)
C33 C34 Ru1	70.4(8)	C36A C35A Ru1A	70.7(10)
C35 C34 H34	126.8	C34A C35A Ru1A	70.9(10)
C33 C34 H34	126.8	C36A C35A H35A	125.3
Ru1 C34 H34	123.2	C34A C35A H35A	125.3
C36 C35 C34	111.3(17)	Ru1A C35A H35A	124.7
C36 C35 Ru1	72.4(8)	C35A C36A C37A	105(3)
C34 C35 Ru1	71.4(8)	C35A C36A Ru1A	71.9(10)
C36 C35 H35	124.4	C37A C36A Ru1A	71.6(10)
C34 C35 H35	124.4	C35A C36A H36A	127.4
Ru1 C35 H35	123.4	C37A C36A H36A	127.4
C35 C36 C37	105.2(16)	Ru1A C36A H36A	121.0

C35 C36 Ru1	70.8(8)	C33A C37A C36A	111(3)
C37 C36 Ru1	71.1(8)	C33A C37A Ru1A	71.0(10)
C35 C36 H36	127.4	C36A C37A Ru1A	70.8(10)
C37 C36 H36	127.4	C33A C37A H37A	124.4
Ru1 C36 H36	122.5	C36A C37A H37A	124.4
C33 C37 C36	109.2(15)	Ru1A C37A H37A	125.3
C33 C37 Ru1	70.0(8)	C37A C36A H36A	127.4
C36 C37 Ru1	71.5(8)	Ru1A C36A H36A	121.0
C33 C37 H37	125.4	C33A C37A C36A	111(3)
C36 C37 H37	125.4	C33A C37A Ru1A	71.0(10)
Ru1 C37 H37	124.7		

### Derivation of the rate law



$$\frac{d[2a]}{dt} = k_2 [CpRu(PPh_3)Cl][PMePh_2] \quad (1)$$

$$\frac{d[CpRu(PPh_3)Cl]}{dt} = 0$$

From the steady state approximation,

$$\frac{d[CpRu(PPh_3)Cl]}{dt} = k_1[1a] - k_{-1}[CpRu(PPh_3)Cl][PPh_3] - k_2[CpRu(PPh_3)Cl][PMePh_2] = 0 \quad (2)$$

Solving for  $[CpRu(PPh_3)Cl]$ :

$$[CpRu(PPh_3)Cl] = \frac{k_1[CpRu(PPh_3)_2Cl]}{k_{-1}[PPh_3] + k_2[PMePh_2]} \quad (3)$$

Substituting the  $[CpRu(PPh_3)Cl]$  into equation (1):

$$\frac{d[2a]}{dt} = \frac{k_1 k_2 [CpRu(PPh_3)_2Cl][PMePh_2]}{k_{-1}[PPh_3] + k_2[PMePh_2]} = -\frac{d[1a]}{dt} \quad (4)$$

Where

$$k_{obs} = \frac{k_1 k_2 [PMePh_2]}{k_{-1}[PPh_3] + k_2[PMePh_2]} \quad (5)$$

Rearranging equation (5):

$$\frac{1}{k_{obs}} = \frac{k_{-1}[PPh_3] + k_2[PMePh_2]}{k_1 k_2 [PMePh_2]} = \frac{k_{-1}[PPh_3]}{k_1 k_2 [PMePh_2]} + \frac{k_2[PMePh_2]}{k_1 k_2 [PMePh_2]} = \frac{k_{-1}[PPh_3]}{k_1 k_2 [PMePh_2]} + \frac{1}{k_1} \quad (6)$$

## References

1. T. Wilczeski, M. Bochenska, and J. F. Bernat, *J. F. J. Organometal. Chem.* 1981, **215**, 87-96.
2. M. I. Bruce, C. Hameister, A. G. Swincer, and R. C. Wallis, *Inorg. Synth.* 1990, **28**, 270.
3. P. M. Treichel and D. A. Komar, *Synth. React. Inorg. Met.-Org. Chem.* 1980, **10**, 205-218.
4. a. P. M. Treichel and P. J. Vincenti, *Inorg. Chem.* 1985, **24**, 228-230; b. P. M. Treichel, D. A. Komar, and P. Vincenti, *Inorg. Chim. Acta* 1984, **88**, 151-152; c. R. J. Haines and A. L. DuPreez, *A. L. J. Organometal. Chem.* 1975, **84**, 357-367.
5. Personal communicationa with Prof. Terry Haas (Tufts University) and Prof. Bruce Foxman (Brandeis University).
6. A. Martinsen and J. Songstad, *Acta Chem. Scandinavica* 1977, **31**, 645-650.
7. J. Songstad and L. J. Stangeland *Acta Chem. Scandinavica* 1970, **24**, 804-808.
8. a. M. J. Verschoor-Kirss, O. Hendricks, L. Renna, D. Hill, and R. U. Kirss, *Dalton Trans.* 2014 **43**, 15221-15227; b. D. Hill, C. Delaney, M. Clark, M. Eaton, B. Hassan, O. Hendricks, D. K. Dang, and R. U. Kirss, *RSC Advances* 2017, **7**, 34425-34434.
9. M. J. Frisch, G. W. Trucks, H. B. Schlegel, G. E. Scuseria, M. A. Robb, J. R. Cheeseman, G. Scalmani, V. Barone, B. Mennucci, G. A. Petersson, H. Nakatsuji, M. Caricato, X. Li, H. P. Hratchian, A. F. Izmaylov, J. Bloino, G. Zheng, J. L. Sonnenberg, M. Hada, M. Ehara, K. Toyota, R. Fukuda, J. Hasegawa, M. Ishida, T. Nakajima, Y. Honda, O. Kitao, H. Nakai, T. Vreven, J. J. A. Montgomery, J. E. Peralta, F. Ogliaro, M. Bearpark, J. J. Heyd, E. Brothers, K. N. Kudin, V. N. Staroverov, T. Keith, R. Kobayashi, J. Normand, K. Raghavachari, A. Rendell, J. C. Burant, S. S. Iyengar, J. Tomasi, M. Cossi, N. Rega, J. M. Millam, M. Klene, J. E. Knox, J. B. Cross, V. Bakken, C. Adamo, J. Jaramillo, R. Gomperts, R. E. Stratmann, O. Yazyev, A. J. Austin, R. Cammi, C. Pomelli, J. W. Ochterski, R. L. Martin, K. Morokuma, V. G. Zakrzewski, G. A. Voth, P. Salvador, J. J. Dannenberg, S. Dapprich, A. D. Daniels, O. Farkas, J. B. Foresman, J. V. Ortiz, J. Cioslowski and D. J. Fox, Gaussian 09 Revision B.01, Gaussian, Inc., Wallingford, CT, 2010.
10. a. N. Godbout, D. R. Salahub, J. Andzelm, and E. Wimmer, *Can. J. Chem.*, 1992, **70**, 560-71; b. C. Sosa, J. Andzelm, B. C. Elkin, E. Wimmer, K. D. Dobbs, and D. A. Dixon, *J. Phys. Chem.*, 1992, **96**, 6630-36
11. a. T. H. Dunning Jr. and P. J. Hay, in *Modern Theoretical Chemistry*, Ed. H. F. Schaefer III, Vol. 3, Plenum, New York, **1977**, 1-28; b. W. R. Wadt and P. J. Hay, *J. Chem. Phys.*, 1985 **82** 284-98; c. P. J. Hay and W. R. Wadt, *J. Chem. Phys.*, 1985, **82**, 299-310; P. J. Hay and W. R. Wadt, *J. Chem. Phys.*, 1985, **82**, 270-83.
12. a. Avogadro: an open-source molecular builder and visualization tool. Version 1.1.1.  
<http://avogadro.openmolecules.net>; b. M. D. Hanwell, D. E. Curtis, D. C. Lonie, T. Vandermeersch, E. Zurek and G. R. Hutchison, *Journal of Cheminformatics* 2012, **4**, 17.
13. a. Gaussian 16, Revision A.03, M. J. Frisch, G. W. Trucks, H. B. Schlegel, G. E. Scuseria, M. A. Robb, J. R. Cheeseman, G.. Scalmani, V. Barone, G. A. Petersson, H. Nakatsuji, X. Li, M. Caricato, A. V. Marenich, J. Bloino, B. G. Janesko, R. Gomperts, B. Mennucci, H. P. Hratchian, J. V. Ortiz, A. F.

Izmaylov, J. L. Sonnenberg, D. Williams-Young, F. Ding, F. Lipparini, F. Egidi, J. Goings, B. Peng, A. Petrone, T. Henderson, D. Ranasinghe, V. G. Zakrzewski, J. Gao, N. Rega, G. Zheng, W. Liang, M. Hada, M. Ehara, K. Toyota, R. Fukuda, J. Hasegawa, M. Ishida, T. Nakajima, Y. Honda, O. Kitao, H. Nakai, T. Vreven, K. Throssell, J. A. Montgomery, Jr., J. E. Peralta, F. Ogliaro, M. J. Bearpark, J. J. Heyd, E. N. Brothers, K. N., Kudin, V. N. Staroverov, T. A. Keith, R. Kobayashi, J. Normand, K. Raghavachari, A. P. Rendell, J. C. Burant, S. S. Iyengar, J. Tomasi, M. Cossi, J. M. Millam, M. Klene, C. Adamo, R. Cammi, J. W. Ochterski, R. L. Martin, K. Morokuma, O. Farkas, J. B. Foresman and D. J. Fox, Gaussian, Inc., Wallingford CT, 2016; b. Y. Zhao and D. G. Truhlar, *Theor Chem Account* 2008, **120**, 215–241.  
<https://doi.org/10.1007/s00214-007-0310-x> c. F. Weigend and R. Ahlrichs, *Phys. Chem. Chem. Phys.* 2005, **7**, 3297-305. d. F. Weigend, *Phys. Chem. Chem. Phys.*, 2006, **8**, 1057-65; e. B. Mennucci, *WIREs Comput. Mol. Sci.* 2012, **2**, 386-404.